

On the Relation of the Deconfinement and the Chiral Phase Transition in Gauge Theories with Fundamental and Adjoint Matter

Jens Braun

*Institut für Kernphysik (Theoriezentrum), Technische Universität Darmstadt,
Schlossgartenstraße 2, D-64289 Darmstadt, Germany and*

Theoretisch-Physikalisches Institut, Friedrich-Schiller-Universität Jena, Max-Wien-Platz 1, D-07743 Jena, Germany

Tina K. Herbst

Institut für Physik, Karl-Franzens-Universität, A-8010 Graz, Austria

We study the relation of confinement and chiral symmetry breaking in gauge theories with non-trivial center, such as $SU(N)$ gauge theories. To this end, we deform these gauge theories by introducing an additional control parameter into the theory and by varying the representation of the quark fields. We then consider a large- $d(R)$ expansion of the effective action, where $d(R)$ denotes the dimension of the representation R of the quark fields. We show how our large- $d(R)$ expansion can be extended in a systematic fashion and discuss the effects of $1/d(R)$ -corrections on the dynamics close to the finite-temperature phase boundary. Our analysis of the fixed-point structure of the theory suggests that the order, in which the chiral and the deconfinement phase transition occur, is dictated by the representation of the quark fields and by the underlying gauge group. In particular, we find that the phase diagram in the plane spanned by the temperature and our additional control parameter exhibits an intriguing phase structure for quarks in the fundamental representation. For $SU(N)$ gauge theories with adjoint quarks, on the other hand, the structure of this phase diagram appears to be less rich, at least in leading order in the $1/d(R)$ -expansion.

I. INTRODUCTION

For quantum chromodynamics (QCD) with $N=3$ colors and two (light) quark flavors it has been found in various studies that the phase transitions associated with chiral symmetry restoration and deconfinement lie remarkably close to each other, see e. g. Refs. [1–16]. From a phenomenological point of view, this observation has important consequences for our understanding of the dynamics in heavy-ion collisions as well as of the generation of hadron masses in the early universe. In fact, a comprehensive picture of the dynamics close to the finite-temperature phase boundary of QCD is required for a reliable description of data from heavy-ion collision experiments [17].

While the underlying mechanisms associated with the confinement of quarks are not yet fully understood, we have a profound understanding of chiral symmetry breaking in gauge theories. In fact, it is already known from Nambu–Jona-Lasinio (NJL) models [18, 19] that chiral symmetry breaking is indicated by strong quark self-interactions. In particular, the four-quark interactions play a prominent role since they are directly related to the chiral order parameter by means of a Hubbard-Stratonovich transformation. Contrary to NJL-type models, however, the quark self-interactions are not free parameters of QCD but generated dynamically and driven to criticality by the gauge degrees of freedom. This can be understood in simple terms from a renormalization group (RG) analysis of the fixed-point structure of four-fermion interactions in gauge theories [20–27]. Such a fixed-point analysis also allows for a computation of the chiral phase transition temperature as a function of

the flavor number N_f , see Refs. [22, 23]. The results are indeed in very good agreement with those from lattice simulations [8–10, 13]. Also in agreement with lattice studies, the deconfinement and chiral phase transition temperature have been found to almost coincide within such a first-principles RG setup [12, 15]. In Ref. [28] it has then been shown that the (almost) coincidence of the chiral and deconfinement phase transition temperature can also be understood by means of an analysis of the influence of gluodynamics on the fermionic fixed-point structure.

In particular with respect to the phase boundary of QCD at finite temperature and quark chemical potential, the interrelation of the chiral and the deconfinement phase transition is currently under debate, see e. g. Ref. [29]. A systematic deformation of QCD represents a valuable strategy to gain important insights into this question. From the response of the theory to such a deformation, we may then learn something about the underlying mechanisms at work. For example, varying the number of quark flavors, the number of colors, or the current quark masses indicates that the nature of the two phase transitions clearly depends on these parameters of the theory, see e. g. Refs. [3, 30–35]. More recently, the interplay of the chiral and deconfinement phase transition has been analyzed by varying the boundary conditions of the quark fields in the temporal direction [36]. Such a deformation of the theory yields so-called dual observables which relate the spectrum of the Dirac operator to the order parameter for confinement, namely the dressed Polyakov loop [12, 37–47].

In this work, we consider a deformation of QCD different from the ones named above. To be specific, we deform QCD by varying the representation of the quark

fields. For example, one may consider quark fields in the adjoint or in the fundamental representation. From such a straightforward deformation it is then possible to gain further insights into the mechanisms close to the finite-temperature phase boundary of QCD. In fact, basic properties of the theory can change when we change the representation of the quark fields: for example, quarks in the adjoint representation do not break the underlying center symmetry of the gauge sector, whereas the center symmetry is broken explicitly for quarks in the fundamental representation. Since center-symmetry breaking is connected to the question of quark confinement [48], one may expect that a variation of the representation of the quark field leaves its imprints in the phase structure of the theory. In fact, it has been found in lattice simulations of $SU(N)$ gauge theory with adjoint quarks [49–51] that the chiral phase transition temperature is significantly larger than the deconfinement phase transition temperature, in contradistinction to QCD with two (light) quark flavors in the fundamental representation. For a study of adjoint QCD with Polyakov-loop extended NJL (PNJL) models, we refer the reader to Refs. [52, 53].

Here we pursue the strategy of Ref. [28] and investigate the fixed-point structure of quark self-interactions. On the one hand, the results of our study provide further insights into the interrelation of quark confinement and chiral symmetry breaking. On the other hand, our fixed-point analysis may help to develop new effective QCD low-energy models or to improve existing models. In this spirit, the present study also extends previous works in which it has been discussed how the low-energy sector of QCD can be systematically connected to the QCD Lagrangian at high momentum scales within a continuum approach [12, 15, 20–24, 54].

This work is organized as follows: In Sect. II we discuss general aspects of our field-theoretical setup, with an emphasis on the order parameters associated with quark confinement and chiral symmetry breaking. The fermionic fixed-point structure is then discussed in detail in Sect. III for general representations of the quark fields. In Sect. IV we study the partially bosonized version of our fermionic ansatz discussed in Sect. III. The mapping between the two formulations is discussed in Sect. IV B. While the purely fermionic formulation of the matter sector already allows us to analyze the mechanisms at work at the phase boundary, the partially bosonized version allows us to gain access to the hadronic spectrum of the theory in a simple manner. In Sect. IV C, we then take into account $1/d(R)$ -corrections and discuss their effect on the finite-temperature phase boundary. Our concluding remarks are given in Sect. V.

II. GENERAL ASPECTS OF QCD AT LOW ENERGIES

In QCD phenomenology, the quarks are usually assumed to live in the fundamental representation of the underlying $SU(N)$ gauge group. In the construction of general gauge theories, however, the quarks are by no means bound to live in the fundamental representation. In principle, they may transform according to any irreducible representation of the $SU(N)$ gauge group, e. g. the fundamental representation (N -dimensional) or the adjoint representation (N^2-1 -dimensional). On the other hand, the gauge degrees of freedom always transform according to the adjoint representation of the gauge group.

In order to analyze the interplay of the chiral and the deconfinement phase transition in QCD, we deform QCD by varying the representation of the quark fields and by adding a relevant coupling to the theory which can be considered as an external deformation parameter. For the latter, we choose a four-fermion coupling $\bar{\lambda}_\psi$:

$$S_{\text{QCD}} \rightarrow S_{\text{QCD}} + \int d^4x \bar{\lambda}_\psi (\bar{\psi} \mathcal{C} \psi)^2,$$

where S_{QCD} denotes the (classical) action of QCD, see e. g. Refs. [55, 56] for lattice studies of this class of theories. The operator \mathcal{C} will be determined below. Loosely speaking, such a deformation allows us to “detune” the chiral and the confining dynamics of the theory. Due to the additional coupling, the theory (“ λ_ψ -deformed QCD”) now effectively depends on two parameters, namely $\bar{\lambda}_\psi$ and Λ_{QCD} .¹ In particular, the values of chiral low-energy observables, depend on these two parameters. Different values of $\bar{\lambda}_\psi$ can then be related to different values of a given low-energy observable, such as the pion decay constant f_π . For $\bar{\lambda}_\psi \equiv 0$, we are left with real QCD and the only input parameter is given by Λ_{QCD} or, equivalently, by the value of the strong coupling α_s at some (high) momentum scale. In this case, Λ_{QCD} solely sets the scale for all physical observables \mathcal{O} : $\mathcal{O} \sim \Lambda_{\text{QCD}}$.²

In the following we would like to exploit the dependence on the two parameters Λ_{QCD} and $\bar{\lambda}_\psi$ to gain insights into the relation of the chiral and the deconfinement phase transition. To this end, we set up a model which shares many aspects with the full theory but can also be analyzed analytically to a large extent. Following Ref. [28], this allows us to come up with a prediction for a phase diagram in the plane spanned by the temperature and the pion decay constant f_π for different representations of the quark fields. This prediction can then be tested with the aid of other approaches, such as lattice simulations.

¹ Here, we assume that the current quark masses are set to zero.

² One could also turn the argument around and, for example, fix the scale by choosing a certain value T_d for the deconfinement phase transition temperature. The latter then determines the scale Λ_{QCD} .

We would like to mention that gauge theories with an additional relevant parameter, such as a four-fermion coupling, have also attracted a lot of attention in recent years in beyond standard model applications, see e. g. Refs. [56, 57]. In particular, the case of SU(2) gauge theory with two adjoint quarks is of interest, see e. g. Refs. [58–61]. With regard to our present study, a word of caution needs to be added at this point. In our numerical analysis in Sects. III and IV we mostly restrict ourselves to the case of SU(2) gauge theory with two massless adjoint quarks. We are aware of the fact that this theory could already lie in the conformal window. In this work, however, we assume that the zero-temperature ground state of SU(2) gauge theory with two adjoint quarks is governed by dynamical chiral symmetry breaking which would indeed appear to be the case within our present approximations. This is in accordance with Refs. [57, 62]. As a first step, it is therefore natural for us to consider this theory in our numerical studies. Even if our present approximations should turn out to be insufficient to describe correctly the chiral ground-state properties of SU(2) gauge theory with two massless adjoint quarks, we still expect that our results will be similar for gauge groups of higher rank and broken chiral symmetry in the zero-temperature limit, see also our discussion in Sects. III and IV.

Before we now study the interplay of the chiral and the deconfinement phase transition in detail, we summarize a few field-theoretical aspects and explain the general setup which underlies our study.

A. Gauge Sector

Since we are interested in an analysis of the relation of the deconfinement and chiral phase transition in general gauge theories (with non-trivial center), such as SU(N) and Sp(N) gauge theories, we need to discuss at least some properties of the order parameters for confinement and chiral symmetry breaking. In the following we first present a few important analytic relations for the confinement order parameter. These relations will play an important role in our classification of gauge theories in the remainder of this work.

The deconfinement phase transition in pure SU(N) gauge theories has been studied in great detail. For example, results are available from lattice simulations, see e. g. Refs. [8–10, 13, 32, 63–69], as well as from functional continuum methods [33, 70, 71]. A well-known order parameter for the deconfinement phase transition is the Polyakov loop. The associated Polyakov-loop variable reads

$$L_{\text{F}}[A_0] = \frac{1}{d(\text{F})} \mathcal{P} e^{i\bar{g} \int_0^\beta dx_0 A_0(x_0, \vec{x})}, \quad (1)$$

where $\beta = 1/T$ is the inverse temperature, $d(\text{F})$ is the dimension of the fundamental representation of the gauge group (e. g. $d(\text{F}) = N$ for SU(N) gauge theories), \bar{g} de-

notes the bare gauge coupling and \mathcal{P} stands for path ordering. The Polyakov loop is then given by $\langle \text{tr}_{\text{F}} L_{\text{F}} \rangle$.

Strictly speaking, the Polyakov loop $\langle \text{tr}_{\text{F}} L_{\text{F}} \rangle$ is an order parameter for center symmetry breaking, see e. g. Ref. [48]. However, its logarithm can also be viewed as half of the free energy $F_{q\bar{q}}$ of a quark-antiquark pair at infinite distance. A center-symmetric confining phase is signaled by a vanishing Polyakov loop and implies that the free energy of a static fundamental quark (fundamental color source) $F_q \simeq (1/2)F_{q\bar{q}}$ is infinite. The associated quark-antiquark potential is linearly rising for large distances in this phase and no string breaking occurs. On the other hand, the deconfined phase is associated with a finite free energy F_q and a finite Polyakov loop, i. e. (spontaneously) broken center symmetry, see below.

Apart from the Polyakov loop, other order parameters for quark confinement have been introduced, such as dual observables [36]. In this work, however, we shall mainly consider an order parameter which is closely related to the standard Polyakov loop, namely $\text{tr}_{\text{F}} L_{\text{F}}[\langle A_0 \rangle]$. In Polyakov-Landau-DeWitt gauge it has indeed been shown that the quantity $\text{tr}_{\text{F}} L_{\text{F}}[\langle A_0 \rangle]$ serves as an order parameter for confinement [70, 71]. Here, $\langle A_0 \rangle$ is a constant element of the Cartan subalgebra of the gauge group and denotes the ground state of the order parameter potential in the adjoint algebra, namely the so-called Polyakov-loop potential.³ In a one-loop approximation this order parameter potential has first been computed in Refs. [72, 73]. Based on a functional RG approach, a non-perturbative study of this potential, including a computation of the phase transition temperatures for several gauge groups, has first been carried out in Refs. [33, 70, 71]. Since the phase transition temperature of a given gauge theory represents a physical quantity, it can be easily compared to results from other approaches, such as lattice gauge theory, see e. g. Refs. [32, 64, 66, 67]. For example, such a comparison shows that the RG result for the deconfinement phase transition temperature T_{d} for SU(3) is in very good agreement with results from lattice simulations.⁴

In the following we shall refer to the temperature T_{d} as the deconfinement phase transition temperature, even if

³ Strictly speaking, we have to distinguish between the background temporal gauge field and its expectation value $\langle A_0 \rangle$ associated with the order parameter for confinement, $\text{tr}_{\text{F}} L_{\text{F}}[\langle A_0 \rangle]$. We skip this subtlety here and refer to $\langle A_0 \rangle$ as the position of the ground-state of the order-parameter potential if not indicated otherwise.

⁴ The deconfinement phase transition has also been studied with matrix models, see e. g. Refs. [35, 74–76]. Based on input from lattice simulations, on the other hand, ways to improve Polyakov-loop potentials widely used in PNJL/PQM-type model studies have been discussed in a recent review, see Ref. [77]. For recent progress in this direction, we refer to Refs. [78, 79]. We emphasize that our present study relies directly on the order-parameter potential spanned by the background temporal gauge field. The position $\langle A_0 \rangle$ of the ground state of this potential appears in the Feynman diagrams associated with the dynamics in the matter sector, see discussion in Sects. II B, III and IV.

we study theories with quarks in a representation other than the fundamental representation. As we shall briefly discuss below, there exist representations for which the associated quark-antiquark potential is not linearly rising at large distances, independent of the temperature T . Below T_d , however, center symmetry is restored also in these cases. In any case, free (static) color charges are always screened to form color-neutral states below T_d for any representation that is considered in this work.

Let us now discuss some important properties of the quantity

$$L_R[A_0] = \frac{1}{d(R)} \mathcal{P} e^{i\bar{g} \int_0^\beta dx_0 A_0(x_0, \vec{x})}. \quad (2)$$

Here, R denotes the representation of the matter fields, e. g. fundamental (F) or adjoint (A), and $d(R)$ is the dimension of the representation R .

Under an arbitrary center transformation of the ground state $\langle A_0 \rangle$,

$$\langle A_0 \rangle \rightarrow \langle A_0 \rangle_z, \quad (3)$$

the quantity $\text{tr}_R L_R[\langle A_0 \rangle]$ transforms as

$$\text{tr}_R L_R[\langle A_0 \rangle] \rightarrow z^{\mathcal{N}_R} \text{tr}_R L_R[\langle A_0 \rangle], \quad (4)$$

where \mathcal{N}_R denotes the so-called N -ality of the representation R . For $SU(N)$ gauge theories, for example, we have

$$z \in \left\{ e^{\frac{2\pi i n}{N}} \right\}_{n=0, \dots, N-1}. \quad (5)$$

Moreover, we have $\mathcal{N}_R = 1$ for $R=F$. We then obtain

$$\text{tr}_F L_F[\langle A_0 \rangle] \rightarrow z \text{tr}_F L_F[\langle A_0 \rangle] \quad (6)$$

and conclude that $\text{tr}_F L_F[\langle A_0 \rangle]$ is an order parameter for center symmetry breaking and, loosely speaking, signals confinement of (static) quarks in the fundamental representation, see our discussion above. Note that $\langle \text{tr}_F L_F[A_0] \rangle$ transforms accordingly under arbitrary center transformations of the gauge field A_0 . Hence, both $\text{tr}_F L_F[\langle A_0 \rangle]$ and $\langle \text{tr}_F L_F[A_0] \rangle$ represent order parameters for center symmetry breaking.

By construction, $\langle A_0 \rangle$ is an element of the Cartan subalgebra. In the following we may therefore parameterize it in terms of the generators of this subalgebra:

$$\beta \bar{g} \langle A_0 \rangle = 2\pi \sum_{a=1}^{d(C)} T^{(a)} \phi^{(a)} = 2\pi \sum_{a=1}^{d(C)} T^{(a)} v^{(a)} |\phi|, \quad (7)$$

where $v^2 = 1$, the $T^{(a)}$'s are the generators of the underlying gauge group in a given representation R . We shall refer to the set $\{\phi^{(a)}\}$ as the coordinates of $\langle A_0 \rangle$.

The center-symmetric phase is signaled by [71]

$$\text{tr}_F L_F[\langle A_0 \rangle] = \langle \text{tr}_F L_F[A_0] \rangle = 0.$$

In the class of Polyakov-DeWitt gauges, it then follows that the position $\langle A_0 \rangle$ of the center symmetric ground state is uniquely determined by [27, 33, 70]

$$\text{tr}_F(L_F[\langle A_0 \rangle]^n) = 0, \quad (8)$$

where $n = 1, \dots, d(C)$ is the dimension of the associated Cartan subalgebra. For $SU(N)$, we have $d(C) = N - 1$. At (asymptotically) high temperatures, on the other hand, we are in the perturbative regime where $\langle A_0 \rangle \rightarrow 0$ and $\text{tr}_F L_F[\langle A_0 \rangle] \rightarrow 1$, see e. g. Refs. [33, 70–73]. Since $\text{tr}_F L_F[\cdot]$ is a monotonic function in the domain defined by the trajectory of $\langle A_0 \rangle$ as a function of the temperature T , the quantity $\text{tr}_F L_F[\langle A_0 \rangle]$ is monotonic and $\text{tr}_F L_F[\langle A_0 \rangle] > 0$ in the phase with broken center symmetry, see also our discussion below.

The coordinates $\{\phi^{(a)}\}$ of the center-symmetric ground state, that are determined by Eq. (8), are given by $\{1/2\}$ for $SU(2)$ Yang-Mills theory and $\{2/3, 0\}$ for $SU(3)$, respectively. From our discussion it is also clear that the order-parameter potential in the adjoint algebra is periodic.⁵ The lengths of the periods in the various directions depend on the eigenvalues of the associated generators $T^{(a)}$. Center transformations of the ground state $\langle A_0 \rangle$ can now be viewed as discrete rotations of the coordinates $\{\phi^{(a)}\}$ around the center symmetric point. For example, we have a reflection symmetry with respect to $\phi = 1/2$ for $SU(2)$. The associated center transformation can then be written as follows:

$$\phi \rightarrow \phi_z = 1 - \phi \quad (9)$$

with $\phi \in [0, 1/2]$. Under such a center transformation, the order parameter transforms according to

$$\begin{aligned} \text{tr}_F L_F[\langle A_0 \rangle] &\equiv \text{tr}_F L_F[\phi] = \cos(\pi\phi) \\ &\rightarrow \text{tr}_F L_F[\langle A_0 \rangle_z] = -\text{tr}_F L_F[\langle A_0 \rangle], \end{aligned} \quad (10)$$

as expected from Eq. (4). Note that we have used Eq. (7) to express $\langle A_0 \rangle$ in terms of ϕ .

For $SU(3)$, center transformations of the ground-state $\langle A_0 \rangle$ can be written as rotations by angles of $2\pi n/3$ around the center-symmetric point $\{2/3, 0\}$, where $n = 0, 1, 2$. Under such transformations, one then finds that the order parameter transforms as given in Eq. (4).

We would like to add that Eq. (8) holds only for the center symmetric ground state $\langle A_0 \rangle$ for $n \bmod N \neq 0$. For $n \bmod N = 0$ and N even, we have

$$\text{tr}_F(L_F[\langle A_0 \rangle]^n) = (-1)^{\frac{n}{N}} \frac{1}{N^{n-1}}. \quad (11)$$

For odd N and $n \bmod N = 0$, on the other hand, we have

$$\text{tr}_F(L_F[\langle A_0 \rangle]^n) = \frac{1}{N^{n-1}}. \quad (12)$$

Let us now turn to representations other than the fundamental one. From Eq. (4), we also observe that there may exist representations R of the gauge group for

⁵ The order-parameter potential is also invariant under discrete rotations about the origin. The corresponding rotation angles are determined by the gauge group under consideration.

which $\text{tr}_R L_R[\langle A_0 \rangle]$ does *not* represent an order parameter for center symmetry breaking. To be specific, we consider $\text{tr}_R L_R[\langle A_0 \rangle]$ for $SU(N)$ and $R=A$ (adjoint representation). Since we have $\mathcal{N}_R = 0$ (zero N -ality) in this case, we find that $\text{tr}_A L_A[\langle A_0 \rangle]$ transforms as

$$\text{tr}_A L_A[\langle A_0 \rangle] \rightarrow \text{tr}_A L_A[\langle A_0 \rangle] \quad (13)$$

under a center transformation. To be more specific, for $SU(2)$, we have

$$\text{tr}_A L_A[\langle A_0 \rangle] \equiv \text{tr}_A L_A[\phi] = \frac{1}{3} [1 + 2 \cos(2\pi\phi)], \quad (14)$$

which is insensitive to arbitrary (center) transformations of $\langle A_0 \rangle$, see Eq. (9). Thus, $\text{tr}_A L_A[\langle A_0 \rangle]$ is not an order parameter for center symmetry breaking, see also Refs. [80, 81].

The insensitivity of $\text{tr}_A L_A[\langle A_0 \rangle]$ and $\langle \text{tr}_A L_A[A_0] \rangle$ with respect to center transformations is related to the fact that quarks in the adjoint representation do not break the underlying center symmetry of the gauge group, in contrast to quarks in the fundamental representation. From a phenomenological point of view, there is indeed no strict notion of confinement of quarks in the adjoint representation, even in the static limit. In this case, (static) quarks can be screened by the gluonic degrees of freedom and form a color-singlet state, as can be seen from the decomposition of the tensor product of two adjoint multiplets. Therefore a quark-antiquark pair at large distances can split up into two singlet states. The associated quark-antiquark potential thus flattens at large distances and does not rise linearly, as it is the case for (static) quarks in the fundamental representation, see e. g. Refs. [49–51, 80, 81] for lattice studies. In particular, the Polyakov-loop $\langle \text{tr}_A L_A[A_0] \rangle$ is finite for all temperatures [80, 81]. Since $\langle \text{tr}_A L_A[A_0] \rangle$ is related to the free energy of a static (adjoint) quark, it follows that the free energy is finite, even in the center symmetric phase at low temperatures. Note that the behavior of the quantities $\langle \text{tr}_A L_A[A_0] \rangle$ and $\text{tr}_A L_A[\langle A_0 \rangle]$ changes qualitatively at $T = T_d$, even though they do not represent order parameters for center symmetry breaking. As we shall discuss below, this is due to the fact that $\langle \text{tr}_A L_A[A_0] \rangle$ and $\text{tr}_A L_A[\langle A_0 \rangle]$ can be related to the order parameters $\langle \text{tr}_F L_F[A_0] \rangle$ and $\text{tr}_F L_F[\langle A_0 \rangle]$, respectively.

Let us close this subsection by summarizing a few useful relations for the quantity $\text{tr}_R L_R[\langle A_0 \rangle]$. First, we note that the order parameter $\text{tr}_F L_F[\langle A_0 \rangle]$ can be related to the standard Polyakov-loop via the *Jensen inequality*. For a given *concave* function $f(\cdot)$, we have $f(\langle \cdot \rangle) \geq \langle f(\cdot) \rangle$. For example, this yields

$$\text{tr}_F L_F[\langle A_0 \rangle] \geq \langle \text{tr}_F L_F[A_0] \rangle \quad (15)$$

for $SU(2)$ and $SU(3)$ gauge theory in the deconfined phase [33, 70, 71]. We emphasize that this inequality does not hold for general gauge groups and representations R , since it requires that $\text{tr}_R L_R[\cdot]$ is a concave function in the relevant domain. Provided that $\langle A_0 \rangle(T)$ lies sufficiently close to the origin (e. g. for sufficiently large

temperatures T), however, the inequality may hold for any gauge group and representation.⁶

In addition to Eq. (15), we have the following two simple but useful inequalities:

$$0 \leq \frac{1}{d(R)} |\text{tr}_R(L_R[\langle A_0 \rangle]^n)| \leq \frac{1}{(d(R))^n}, \quad (16)$$

which follows from the generalized triangle inequality, and

$$-\frac{1}{(d(R))^n} \leq \frac{1}{d(R)} \Re[\text{tr}_R(L_R[\langle A_0 \rangle]^n)] \leq \frac{1}{(d(R))^n} \quad (17)$$

for $n \in \mathbb{N}$.

Finally, we evaluate the quantity $\text{tr}_R L_R[\langle A_0 \rangle]$ for specific configurations of the ground-state $\langle A_0 \rangle$. At very high temperatures $T \gg T_d$, we have $\langle A_0 \rangle \rightarrow 0$ and $\text{tr}_R L_R[\langle A_0 \rangle] \rightarrow 1$, independent of the gauge group and the representation R . In the low-temperature phase ($T < T_d$), however, the value of $\text{tr}_R L_R[\langle A_0 \rangle]$ depends on the gauge group and the representation R . For example, we have $\text{tr}_F L_F[\langle A_0 \rangle] = 0$ for $SU(N)$ gauge theories for $T < T_d$. For the adjoint representation, on the other hand, we find

$$\text{tr}_A(L_A[\langle A_0 \rangle]^n) = -\frac{1}{(d(A))^n} = -\frac{1}{(N^2 - 1)^n} \quad (18)$$

with $n \bmod N \neq 0$. For $n \bmod N = 0$, we have

$$\text{tr}_A(L_A[\langle A_0 \rangle]^n) = \frac{1}{(d(A))^{n-1}}. \quad (19)$$

In $SU(N)$ gauge theories, the relation (18) follows straightforwardly from the fact that the tensor product of the triplet and the anti-triplet can be decomposed into the adjoint multiplet and a singlet, $N \otimes \bar{N} = (N^2 - 1) \oplus 1$. Using that the character of the product representation is given by the product of the characters of the representations, we find

$$d(A) \text{tr}_A(L_A[\langle A_0 \rangle]) = |d(F) \text{tr}_F(L_F[\langle A_0 \rangle])|^2 - 1, \quad (20)$$

and similar relations for $\text{tr}_A(L_A[\langle A_0 \rangle]^n)$ with $n > 1$ ($n \in \mathbb{N}$).

Up to this point, we have discussed that below T_d the quantity $\text{tr}_R L_R[\langle A_0 \rangle]$ is zero for $R=F$ but negative for $R=A$. Depending on the representation R , however, it can also assume positive values in the center symmetric phase. For example, let us consider the ten-dimensional representation ($R = \mathbf{10}$) of $SU(3)$. We then find⁷

$$\begin{aligned} d(\mathbf{10}) \text{tr}_{\mathbf{10}}(L_{\mathbf{10}}[\langle A_0 \rangle]) \\ = [d(F) \text{tr}_F(L_F[\langle A_0 \rangle])]^3 \\ - 2 |d(F) \text{tr}_F(L_F[\langle A_0 \rangle])|^2 + 1 = 1 \end{aligned} \quad (21)$$

⁶ In general, a subdomain around the origin can be found such that $\text{tr}_R L_R[\cdot]$ is a concave function. For a more detailed discussion of the relation (15) between the order parameters $\text{tr}_F L_F[\langle A_0 \rangle]$ and $\langle \text{tr}_F L_F[A_0] \rangle$, we refer the reader to Ref. [28].

⁷ Here, we have used that the tensor product of the triplet and the sextet can be decomposed into a singlet and decuplet. Moreover, the tensor product of two triplets can be decomposed into a sextet and an anti-triplet.

for $T < T_d$, and similar relations for $\text{tr}_{10}(L_{10}[\langle A_0 \rangle]^n)$ with $n > 1$ ($n \in \mathbb{N}$). Note that the N -ality of the ten-dimensional representation of $SU(3)$ is zero as well, $\mathcal{N}_{10} = 0$. We add that also higher-dimensional representations exist for which we have $\text{tr}_R L_R[\langle A_0 \rangle] = 0$ for $T < T_d$, even if the N -ality of the representation is zero.

Depending on the representation R , we have seen that the quantity $\text{tr}_R L_R[\langle A_0 \rangle]$ can be zero, positive or negative in the center symmetric phase, i. e. for $T < T_d$. This allows us to classify gauge theories. In Sect. III, we shall see that this classification is to some extent related to the question whether the chiral phase transition temperature is larger or smaller than the deconfinement phase transition in a given gauge theory.

B. Matter Sector

Let us now discuss our field-theoretical setup in the matter sector. Up to this point, our statements concerning the pure gauge sector are exact and can be obtained analytically. They only rely on the basic assumption that we work in the class of Polyakov-DeWitt gauges. For our analysis of the matter sector, we employ the following ansatz for the quantum effective action Γ :

$$\Gamma[\bar{\psi}, \psi, \langle A_0 \rangle] = \int d^4x \left\{ Z_\psi \bar{\psi} (i\cancel{\partial} + \bar{g}\gamma_0 \langle A_0 \rangle) \psi + \frac{\bar{\lambda}_\psi}{2} [(\bar{\psi}\psi)^2 - (\bar{\psi}\vec{\tau}\gamma_5\psi)^2] \right\}, \quad (22)$$

where Z_ψ is the wave-function renormalization of the quark fields. In the present work, we restrict ourselves to $N_f = 2$ massless quark flavors with $d(R)$ colors. The τ_i 's represent the Pauli matrices and couple the spinors in flavor space.

Our ansatz (22) for the matter sector is *perturbatively* non-renormalizable, as it is the case for the NJL model. Therefore we define it with an UV cutoff Λ which then represents an additional parameter of the model. This setup also implies that the regularization scheme belongs to the definition of the model. The role of Λ for the fixed-point structure will be discussed in detail in Sect. IV.

For our study of the RG flow of the four-fermion coupling $\bar{\lambda}_\psi$, we employ the so-called Wetterich equation [82]. The latter is an RG equation for the quantum effective action. In this approach, the effective action Γ depends on the RG scale k (infrared cutoff scale) which determines the RG ‘time’ $t = \ln(k/\Lambda)$ with Λ being a UV cutoff scale. For reviews on and introductions to this functional RG approach, we refer the reader to Refs. [27, 83–92].

Concerning the background field $\langle A_0 \rangle$, we will *not* make use of the approximation $\text{tr}_R L_R[\langle A_0 \rangle] = \langle \text{tr}_R L_R[A_0] \rangle$ which underlies most PNJL/PQM model

studies,⁸ see e. g. Refs. [1, 4, 5, 7, 11, 14, 52, 74, 94–97]. Although this assumption is convenient and opens up the possibility to incorporate lattice results for $\langle \text{tr}_R L_R[A_0] \rangle$, it may be problematic in quark representations other than the fundamental one and away from the limit of infinitely many colors, $d(R) \rightarrow \infty$, see our discussion below. For our analytic studies, we shall rather make use of the exact relations given in Sect. II A. For our numerical evaluation of the quantum effective action, we then use the numerical results for $\langle A_0 \rangle$ from a non-perturbative first-principles RG study of the associated order parameter potential in Polyakov-Landau-DeWitt gauge, see Refs. [33, 70]. Since it has been found for fundamental matter that PNJL/PQM-type model studies are sensitive to different parameterizations of the potential for $\langle \text{tr}_F L_F[A_0] \rangle$, see e. g. Ref. [98], it is in fact important to analyze at least some of the consequences arising from the approximation $\text{tr}_R L_R[\langle A_0 \rangle] = \langle \text{tr}_R L_R[A_0] \rangle$ underlying these model studies.

In general, our ansatz (22) in the matter sector can be considered as the leading order in a systematic derivative expansion. The associated expansion parameter is the anomalous dimension $\eta_\psi = -\partial_t \ln Z_\psi$ of the quark fields. This ‘parameter’ is small as has been found in various previous studies [20, 24, 99, 100]. In fact, it is identical to zero when we consider the four-fermion coupling in the so-called point-like limit, $\lambda_\psi(|p| \ll k)$, see e. g. Ref. [27]. This is true even if we had allowed for dynamical gauge degrees, provided that one considers the class of Landau gauges [101], such as Polyakov-Landau-DeWitt gauge. As we have discussed above, the latter gauge is implicitly assumed in our work, see Sect. II A.

Apart from an expansion in derivatives, the effective action can be expanded in operators, such as n -fermion operators. Regarding four-fermion operators, we note that our ansatz (22) for the effective action is not complete with respect to Fierz transformations even in the limits $\langle A_0 \rangle \rightarrow 0$ and $T \rightarrow 0$, see e. g. Refs. [21–23, 27, 101]. For example, we have dropped a so-called axial-vector channel interaction which would also contribute to the RG flow of our coupling $\bar{\lambda}_\psi$ associated with a scalar-pseudoscalar channel. From a consideration of a Fierz-complete basis, however, we only expect quantitative corrections to our results presented here. The main qualitative aspects are expected to persist since the general structure of the loop integrals remains unchanged [28]. For a Fierz-complete study of RG flow of four-fermion couplings in QCD, we refer the reader to Refs. [21–23, 25, 27, 101]. Regarding the role of higher fermion operators, e. g. 8-fermion operators, we note that it can be shown that these operators do not contribute to the RG flow of the four-fermion couplings in the point-like limit [27]. Beyond the point-like limit, however, these

⁸ Note that there are also PNJL/PQM-type model studies which do not use this approximation but consider an integration over the group $SU(N)$, see e. g. Refs. [6, 93].

higher-order operators may very well contribute to the flow of the four-fermion interactions, see, e. g., our discussion in Sect. IV and Ref. [27].

In the subsequent section we will show that the purely fermionic formulation of our ansatz (22) for the matter sector is convenient for a general discussion of the interplay of the chiral and the deconfinement phase transition, independent of the fermion representation. In order to compute low-energy observables, however, a purely fermionic formulation may not be the first choice since this requires to resolve the momentum-dependence of the fermionic vertices. In this case, a partially bosonized formulation of our ansatz (22) might be better suited. Such a formulation of the effective action can be obtained straightforwardly from a Hubbard-Stratonovich transformation of the underlying path integral and yields

$$\Gamma_k[\bar{\psi}, \psi, \bar{\Phi}, \langle A_0 \rangle] = \int d^4x \left\{ Z_\psi \bar{\psi} (i\partial\!\!\!/ + \bar{g}\gamma_0 \langle A_0 \rangle) \psi \quad (23) \right. \\ \left. + \frac{1}{2} Z_\Phi (\partial_\mu \bar{\Phi})^2 + i\bar{h}\bar{\psi}(\sigma + i\vec{\tau} \cdot \vec{\pi}\gamma_5)\psi + \frac{1}{2}\bar{m}^2 \bar{\Phi}^2 \right\},$$

where the auxiliary bosonic fields $\bar{\Phi}^T = (\sigma, \vec{\pi})$ mediate the interaction between the fermions. Here, we consider these bosons to be composites of fermions which do not carry any internal color or flavor charges: $\sigma \sim (\bar{\psi}\psi)$ and $\vec{\pi} \sim (\bar{\psi}\vec{\tau}\gamma_5\psi)$. Chiral symmetry breaking is now signaled by a non-vanishing expectation value of the σ field. Since the mass parameter \bar{m}^2 describes the curvature of the chiral order parameter potential at the origin, the sign of \bar{m}^2 is related to the question whether chiral symmetry is broken in the ground state or not. For $\bar{m}^2 < 0$, we necessarily have $\langle \sigma \rangle \neq 0$.

In the following we choose the initial conditions for the various couplings in Eq. (23) such that

$$\lim_{k \rightarrow \Lambda} \bar{m}^2 > 0, \quad \lim_{k \rightarrow \Lambda} Z_\Phi = 0, \quad \lim_{k \rightarrow \Lambda} Z_\psi = 1.$$

Together with the identity

$$\bar{\lambda}_\psi = \frac{\bar{h}^2}{\bar{m}^2}, \quad (24)$$

the ansatz (23) can then be mapped onto the ansatz (22) at the initial UV scale Λ . Thus, only the ratio of the Yukawa coupling \bar{h} and the mass parameter \bar{m} acquires a physical meaning. In particular, we observe that a large (i. e. diverging) four-fermion coupling signals the onset of chiral symmetry breaking, since it can be related to a change in the sign of the parameter \bar{m}^2 . In fact, the two criteria are equivalent in the large- $d(\mathbf{R})$ limit due to the absence of fluctuation effects of the Goldstone modes [27]. In any case, we conclude that the fixed-point structure of the coupling $\bar{\lambda}_\psi$ (or, equivalently, of the couplings \bar{m} and \bar{h}) is directly linked to the question of chiral symmetry breaking in the IR limit. In the following we analyze how this fixed-point structure is related to the order parameter for center-symmetry breaking, namely $\text{tr}_F L_F[\langle A_0 \rangle]$. This will eventually allow us to gain insights into the relation of chiral symmetry breaking and center-symmetry breaking at finite temperature.

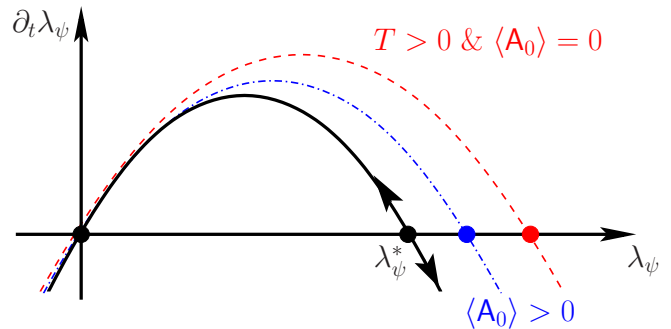


Figure 1. Sketch of the β_{λ_ψ} -function of the four-fermion coupling λ_ψ for vanishing temperature (black/solid line), finite temperature and $\langle A_0 \rangle = 0$ (red/dashed line), and finite temperature and $\langle A_0 \rangle > 0$ (blue/dashed-dotted line), see Eq. (25). The arrows indicate the direction of the RG flow towards the infrared. The figure has been taken from Ref. [27].

III. DYNAMICAL LOCKING MECHANISM AND THE FERMIONIC FIXED-POINT STRUCTURE

Let us begin with an analysis of the interplay of center symmetry breaking and chiral symmetry breaking using the purely fermionic formulation of the effective action, see Eq. (22). Our discussion follows closely the analysis in Ref. [28], where the deformation of the fermionic fixed-point structure due to the presence of confining dynamics has been analyzed for fundamental quarks in detail.

In our study we consider the value of the background field $\langle A_0 \rangle$ as an external input which is given by the ground state of the corresponding order parameter potential. As discussed above, the position $\langle A_0 \rangle$ of the ground state is then directly related to our order parameter for center-symmetry breaking, namely $\text{tr}_F L_F[\langle A_0 \rangle]$. Along the lines of Ref. [28], the RG flow equation of the four-fermion coupling in the point-like approximation can be computed for quarks living in any representation \mathbf{R} . We find

$$\beta_{\lambda_\psi} \equiv \partial_t \lambda_\psi = (2 + 2\eta_\psi) \lambda_\psi \quad (25) \\ - \frac{2}{\pi^2} \left(2 + \frac{1}{d(\mathbf{R})} \right) \sum_{l=1}^{d(\mathbf{R})} l_1^{(\mathbf{F})}(\tau, 0, \nu_l^{(\mathbf{R})} | \phi |) \lambda_\psi^2,$$

where the dimensionless renormalized coupling λ_ψ is defined as

$$\lambda_\psi = Z_\psi^{-2} k^2 \bar{\lambda}_\psi. \quad (26)$$

For example, we have $d(\mathbf{R} = \mathbf{F}) = N$ for quarks in the fundamental representation and $d(\mathbf{R} = \mathbf{A}) = N^2 - 1$ for quarks in the adjoint representation. For convenience, we have introduced the eigenvalues ν_l of the hermitian matrix given in Eq. (7):

$$\nu_l^{(\mathbf{R})} = \text{spec} \{ (T^a v^a)_{ij} \mid v^2 = 1 \}. \quad (27)$$

The coupling λ_ψ depends on the background field $\langle A_0 \rangle$ and the dimensionless temperature $\tau = T/k$. The threshold function $l_1^{(F)}$ describes a regularized one-particle irreducible (1PI) Feynman diagram with two internal

fermion lines. The definition of this function can be found in, e.g., Ref. [28].

The RG flow equation (25) has two fixed-points:⁹ a Gaussian fixed-point ($\lambda_\psi \equiv 0$) and a non-trivial fixed-point $\lambda_\psi^*(\tau, \langle A_0 \rangle)$, see Fig. 1. The non-Gaussian fixed-point can also be computed analytically:¹⁰

$$\begin{aligned} \lambda_\psi^*(\tau, \langle A_0 \rangle) &= \left(\frac{1}{\pi^2} \left(2 + \frac{1}{d(\mathbf{R})} \right) \sum_{l=1}^{d(\mathbf{R})} l_1^{(F)}(\tau, 0, \nu_l^{(\mathbf{R})} | \phi |) \right)^{-1} \\ &= \lambda_\psi^*(0, 0) \left(1 + \frac{1}{d(\mathbf{R})} \sum_{n=1}^{\infty} (-d(\mathbf{R}))^n \left[\text{tr}_{\mathbf{R}}(L_{\mathbf{R}}[\langle A_0 \rangle]^n) + \text{tr}_{\mathbf{R}}(L_{\mathbf{R}}^\dagger[\langle A_0 \rangle]^n) \right] \left(1 + \frac{n}{\tau} \right) e^{-\frac{n}{\tau}} \right)^{-1}, \end{aligned} \quad (28)$$

where

$$\lambda_\psi^* \equiv \lambda_\psi^*(0, 0) = \frac{6\pi^2}{(2d(\mathbf{R}) + 1)}. \quad (29)$$

Thus, we have $d(\mathbf{R})\lambda_\psi^* \rightarrow \text{const.}$ for $d(\mathbf{R}) \rightarrow \infty$. Note that we have dropped terms depending on η_ψ on the right-hand side of Eq. (28). As discussed above, this is not an approximation in the point-like limit.

Before we turn to the case of finite temperature, we briefly discuss a few basic aspects of the zero-temperature limit. In order to solve the RG flow equation (25), we have to choose an initial value λ_ψ^{UV} at the scale $k = \Lambda$ for the coupling λ_ψ . For $\lambda_\psi^{\text{UV}} < \lambda_\psi^*$, we find that the four-fermion coupling approaches the Gaussian fixed-point in the IR limit, i. e. the theory becomes non-interacting and chiral symmetry remains intact. For $\lambda_\psi^{\text{UV}} > \lambda_\psi^*$, on the other hand, we observe that the four-fermion coupling grows rapidly and diverges at a finite scale k_{SB} . This scale signals the onset of chiral symmetry breaking. Below this scale, the point-like approximation is no longer justified: the formation of a quark condensate and the appearance of Nambu-Goldstone modes requires that we resolve the momentum dependence of the four-fermion coupling in this regime. For example, this can be done by means of partial bosonization techniques, see Sect. IV. In any case, the chiral symmetry breaking scale k_{SB} sets

the scale for all chiral low-energy observables \mathcal{O} :

$$\mathcal{O} \sim k_{\text{SB}}^{d_{\mathcal{O}}} \sim \left[1 - \left(\frac{\lambda_\psi^*}{\lambda_\psi^{\text{UV}}} \right) \right]^{\frac{d_{\mathcal{O}}}{|\Theta|}} \theta(\lambda_\psi^{\text{UV}} - \lambda_\psi^*), \quad (30)$$

where $d_{\mathcal{O}}$ is the canonical mass dimension of the observable \mathcal{O} and the critical exponent Θ is defined as

$$\Theta = - \left. \frac{\partial \beta_{\lambda_\psi}}{\partial \lambda_\psi} \right|_{\lambda_\psi^*} = 2. \quad (31)$$

For details, we refer the reader to Ref. [27]. In the following we fix $\lambda_\psi^{\text{UV}} > \lambda_\psi^*$ at $T = 0$. The value of λ_ψ^{UV} then determines the symmetry breaking scale k_{SB} and, in turn, the values of the chiral low-energy observables. For our study of finite-temperature effects and effects from the confining dynamics parameterized by the background field $\langle A_0 \rangle$, we leave our choice for λ_ψ^{UV} unchanged. This ensures comparability of our results at zero and finite temperature for a theory defined by a given value of λ_ψ^{UV} .

At finite temperature and finite $\langle A_0 \rangle$, the fixed-point structure of the theory is deformed compared to the zero-temperature limit. For illustration purposes, we begin with a brief discussion of the case with vanishing gluonic background field. In this case, the pseudo fixed-point is shifted to larger values at finite temperature, $\lambda_\psi^*(\tau, 0) > \lambda_\psi^*$, see Eq. (28). For a given initial value $\lambda_\psi^{\text{UV}} > \lambda_\psi^*$, this implies that a critical temperature T_χ exists above which chiral symmetry is restored, see Ref. [27] for a detailed discussion. Strictly speaking, the critical temperature T_χ is defined to be the temperature for which $1/\lambda_\psi \rightarrow 0$ for $k \rightarrow 0$. From the RG flow equation (25), one then obtains a simple analytic expression for T_χ :

$$T_\chi = \left(\frac{\Lambda}{\pi} \right) \left[1 - \left(\frac{\lambda_\psi^*}{\lambda_\psi^{\text{UV}}} \right) \right]^{\frac{1}{2}} \theta(\lambda_\psi^{\text{UV}} - \lambda_\psi^*), \quad (32)$$

which is accordance with our general statement in Eq. (30). To derive this expression, we have assumed that $T/\Lambda \ll 1$.

⁹ At finite temperature, the non-Gaussian fixed-point is rather a pseudo fixed-point, i. e. the fixed-point inherits an implicit scale dependence from the dimensionless temperature $\tau = T/k$ as well as a dependence on $\langle A_0 \rangle$. Moreover, the line of pseudo fixed-points $\lambda_\psi^*(\tau, \langle A_0 \rangle)$ does not represent a separatrix in the (λ_ψ, τ) -plane. However, it represents a strict upper bound for the separatrix in this plane [27].

¹⁰ The fixed-point value is not a universal quantity as can be seen from its dependence on the regularization scheme. However, the statement about the existence of the fixed-point and its qualitative dependence on the temperature and $\langle A_0 \rangle$ is universal.

Let us now turn to the case of finite $\langle A_0 \rangle$. For fermions in the fundamental representation, for example, we have $\text{tr}_F(L_F[\langle A_0 \rangle]^n) \rightarrow 0$ in the center symmetric phase for $n \in \mathbb{N}$ and $d(F) = N \rightarrow \infty$, see Eq. (8). Thus, the temperature-dependent corrections to $\lambda_\psi^*(\tau, \langle A_0 \rangle)$ vanish identically and we have $\lambda_\psi^*(\tau, \langle A_0 \rangle) \equiv \lambda_\psi^*(0, 0)$ for $T \leq T_d$. We shall refer to this as a locking mechanism for the chiral phase transition [28]. Loosely speaking, this means that the chiral phase transition is locked in due to the confining dynamics. For $T > T_d$, we have $\text{tr}_F L_F[\langle A_0 \rangle] > 0$ and the fixed-point is again shifted to larger values. As pointed out in Ref. [28], this implies that $T_\chi \geq T_d$ in the limit $N \rightarrow \infty$, see also Refs. [1, 102]. In the case of adjoint fermions and $d(R) \gg 1$, the temperature-dependent corrections in Eq. (28) do not vanish identically on all RG scales k for $T \leq T_d$ since we now have $\text{tr}_A(L_A[\langle A_0 \rangle]^n) < 0$ for these temperatures, see Eq. (18). Therefore the (global) sign of the temperature-dependent corrections changes compared to the case with $\langle A_0 \rangle = 0$. This implies that the pseudo fixed-point is shifted to smaller values at finite temperature rather than to larger values.¹¹ For fixed T and $k \rightarrow 0$ (i. e. $\tau \rightarrow \infty$), the pseudo fixed-point approaches

$$\lambda_\psi^*(\tau \rightarrow \infty, \langle A_0 \rangle) = \frac{\lambda_\psi^*}{1 + \frac{1}{d(A)}}. \quad (33)$$

For $d(A) \rightarrow \infty$, we have $\lambda_\psi^*(\tau \rightarrow \infty, \langle A_0 \rangle) \rightarrow \lambda_\psi^*$ from below. Since $\text{tr}_A L_A[\langle A_0 \rangle] \rightarrow 1$ for $T \gg T_d$, the fixed-point is “released” and shifted to larger values. For a given initial value $\lambda_\psi^{\text{UV}} > \lambda_\psi^*$, it then follows again that $T_\chi \geq T_d$ for $d(A) \rightarrow \infty$.

This analysis can in principle be repeated for any fermion representation, including fermion representations for which $\text{tr}_R L_R[\langle A_0 \rangle] > 0$ for $T < T_d$, such as the ten-dimensional representation, see Eq. (21). In the latter case, the temperature-dependent corrections do not vanish for large values of $d(R)$. However, the finite-temperature shift of the fixed-point is still suppressed by a factor of $1/d(R)$ compared to the case with $\langle A_0 \rangle = 0$. As a consequence, the chiral phase transition temperature is increased, but it is not necessarily pushed above the deconfinement phase transition temperature. Therefore a strict statement about the relation of the chiral and the deconfinement phase transition cannot be made for this class of theories, not even in the large- $d(R)$ limit.

From Eq. (25), we can derive an implicit equation for the chiral phase transition temperature T_χ provided that we neglect a possible RG scale dependence of $\text{tr}_R L_R[\langle A_0 \rangle]$:

$$T_\chi^2 = \frac{1}{\mathcal{P}_R(T_\chi)} \left(\frac{\Lambda}{\pi} \right)^2 \left[1 - \left(\frac{\lambda_\psi^*}{\lambda_\psi^{\text{UV}}} \right) \right] \theta(\lambda_\psi^{\text{UV}} - \lambda_\psi^*), \quad (34)$$

where

$$\mathcal{P}_R(T) = -\frac{6}{d(R)\pi^2} \sum_{n=1}^{\infty} \frac{1}{n^2} (-d(R))^n [\text{tr}_R(L_R[\langle A_0 \rangle]^n) + \text{tr}_R(L_R^\dagger[\langle A_0 \rangle]^n)]. \quad (35)$$

In order to derive this equation, we have again assumed that $T/\Lambda \ll 1$. For $\langle A_0 \rangle \rightarrow 0$, we have $\mathcal{P}_R(T) = 1$, as expected from Eq. (32). Since $\text{tr}_R L_R[\langle A_0 \rangle]$ depends on T_d , Eq. (34) relates the chiral phase transition temperature T_χ to the deconfinement phase transition temperature T_d .

For fermions in the fundamental representation and $N \rightarrow \infty$, we have $\mathcal{P}_F(T) = 0$ for $T \leq T_d$ and $\mathcal{P}_F(T) > 0$ for $T > T_d$. Thus, no finite solution of Eq. (34) exists for $T_\chi < T_d$. In accordance with our fixed-point analysis, we conclude that $T_\chi \geq T_d$.

For fermions in the adjoint representation and $d(A) \gg 1$, we have $\mathcal{P}_A(T) \approx -1/d(A)$ for $T \leq T_d$. As in the case of fundamental matter fields, this implies again that $T_\chi \geq T_d$. For fermion representations with $0 < \mathcal{P}_R(T) < 1$ for $T < T_d$, we observe that the chiral phase transition temperature is still shifted to larger values compared to the case with $\langle A_0 \rangle = 0$. However, a definite statement about the temperature-order of the two phase transitions cannot be made in this case.

Let us now turn to the case of finite values of $d(R)$. For fermions in the fundamental representation, we then find $\mathcal{P}_F(T) = 1/N^2 > 0$ for $T \leq T_d$. For $T > T_d$, $\mathcal{P}_F(T)$ increases monotonically from $\mathcal{P}_F(T_d) = 1/N^2$ to $\mathcal{P}_F(T \rightarrow \infty) \rightarrow 1$. In fact, right above the deconfinement phase transition, the quantity $\mathcal{P}_F(T)$ increases rapidly since $\text{tr}_F L_F[\langle A_0 \rangle]$ increases rapidly. Since $\mathcal{P}_F(T)$ is finite for all temperatures, we find a regime where $T_\chi < T_d$ for $\lambda_\psi^{\text{UV}}/\lambda_\psi^* \gtrsim 1$. In the left panel of Fig. 2, we show our numerical results for T_χ/T_d as a function of $\lambda_\psi^{\text{UV}}/\lambda_\psi^*$. For larger values of $\lambda_\psi^{\text{UV}}/\lambda_\psi^*$, a window in parameter space opens up in which the chiral and the deconfinement phase transition (almost) coincide. In the limit $N \rightarrow \infty$, this locking window extends down to $\lambda_\psi^{\text{UV}}/\lambda_\psi^* = 1$, as illustrated by a comparison of our results for $N = 2$ and $N = 3$ in Fig. 2. Note that the locking window for $\lambda_\psi^{\text{UV}}/\lambda_\psi^*$ can be related to a locking window for low-energy observables, such as the pion decay constant. We shall come back to this in Sect. IV.

In case of adjoint fermions and finite $d(A)$, we have $\mathcal{P}_A(T) \leq 0$ for $T \leq T_d$. For example, we have $\mathcal{P}_A(T) = -1$ for $N = 2$. For $T \gtrsim T_d$, $\mathcal{P}_A(T)$ increases rapidly and changes its sign. For $T \gg T_d$, it then approaches $\mathcal{P}_A(T) = 1$. Since we have $\mathcal{P}_A(T) \leq 0$ even for finite N , we find that the chiral phase transition temperature is larger than the deconfinement phase transition temperature, independent of our choice for $\lambda_\psi^{\text{UV}}/\lambda_\psi^* > 1$ and $N \geq 2$, see right panel of Fig. 2 for our numerical results for $N = 2$. Note that this observation is compatible with lattice results of SU(2) gauge theory with two adjoint quarks, see Refs. [49–51]. In our analysis, it

¹¹ Note that an external magnetic field deforms the fixed-point structure in a similar way [103, 104].

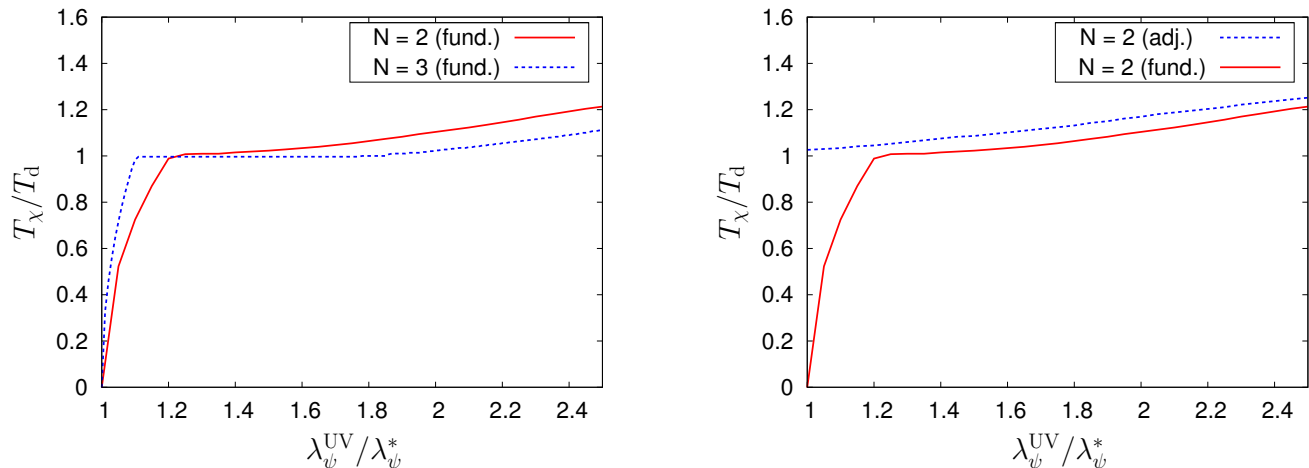


Figure 2. Left panel: Phase diagram in the plane spanned by the temperature and the rescaled coupling $\lambda_\psi^{\text{UV}}/\lambda_\psi^*$ for $N_f = 2$ massless quark flavors in the fundamental representation and $N = 2$ colors (red/solid line) as well as for $N = 3$ colors (blue/dashed line), see also Ref. [28]. Note that there is no splitting of the phase boundary (i. e. $T_\chi \simeq T_d$) for small λ_ψ^{UV} in the large- N limit, see Eq. (34) and discussion thereof. Right panel: T_χ/T_d as a function of $\lambda_\psi^{\text{UV}}/\lambda_\psi^*$ for $N_f = 2$ massless quarks in the fundamental representation ($N = 2$) (red/solid line) as well as for quarks in the adjoint representation (blue/dashed line).

can be traced back to the deformation of the fermionic fixed-point structure in the presence of gauge dynamics.

To obtain the numerical results in Fig. 2, we have employed data for $\langle A_0 \rangle(T)$ as obtained from an RG study of the associated order parameter potential for SU(2) and SU(3) Yang-Mills theory [33, 70]. However, we did not take into account the back-reaction of the matter fields on the order parameter potential associated with $\langle A_0 \rangle$. In the case of fundamental matter, we expect that this back-reaction will shrink the size of the locking window since it further increases the quantity $\mathcal{P}_F(T)$ at low temperatures. For adjoint quarks, the back-reaction will also increase $\mathcal{P}_A(T)$. Nevertheless, it may remain negative over a wide range of temperatures. Therefore we may still have $T_\chi > T_d$ for all values of $\lambda_\psi^{\text{UV}}/\lambda_\psi^* > 1$, at least for $N = 2$.

Let us add a word of caution on the treatment of the quantity $\text{tr}_R L_R[\langle A_0 \rangle]$ in standard PNJL/PQM model approaches. In these studies, one relies on the assumption that $\text{tr}_R L_R[\langle A_0 \rangle] = \langle \text{tr}_R L_R[A_0] \rangle$. For $\langle \text{tr}_R L_R[A_0] \rangle$, one then uses lattice data as input. Whereas such an approach would lead to similar conclusions for fundamental quarks ($\langle \text{tr}_F L_F[A_0] \rangle \geq 0$ and $\text{tr}_F L_F[\langle A_0 \rangle] \geq 0$), the situation is different for adjoint quarks. In the latter case, we have $\langle \text{tr}_A L_A[A_0] \rangle > 0$ but $\text{tr}_A L_A[\langle A_0 \rangle]$ can assume both positive and negative values as discussed above.

Before we now enter the discussion of the RG flows of the partially bosonized formulation of the matter sector, we would like to comment on the number of parameters in our study. Up to this point, our discussion suggests that our study only relies on a single parameter in the matter sector apart from the UV cutoff Λ , namely on the initial value λ_ψ^{UV} . Strictly speaking, however, the non-trivial fixed-point of the four-fermion interaction is an artifact of our point-like approximation. With the aid

of the partially bosonized formulation, we will resolve part of the momentum dependence of the four-fermion interaction. We will then find that the matter sector depends on three parameters: the Yukawa coupling \bar{h} , the bosonic mass parameter \bar{m} and the UV cutoff Λ , see Eq. (23). This is a substantial difference to, e. g., fermion models in $d < 4$ space-time dimensions, where we only have a single parameter in both formulations, see e. g. Ref. [105]. There, the non-trivial fixed-point of the four-fermion coupling can be mapped onto a corresponding non-trivial fixed-point in the plane spanned by the renormalized Yukawa coupling h and the dimensionless renormalized bosonic mass parameter m . In our case, the role of the non-trivial fixed-point in the purely fermionic formulation is taken over by a separatrix in the (h^2, m^2) -plane in the partially bosonized formulation. The shift of the non-trivial fixed-point of the four-fermion coupling due to the gauge dynamics then turns into a corresponding shift of this separatrix. The mapping between the two formulations is discussed in detail in the subsequent section. Being aware of this subtlety, the discussion of the fermionic fixed-point structure is still useful and nicely illustrates the mechanism underlying the interplay of the chiral and the deconfinement phase transition.

IV. PARTIAL BOSONIZATION AND THE LARGE- $d(R)$ EXPANSION

A. Gap Equation

In this subsection, we briefly discuss how our study of fermionic RG flows is related to the gap equation for the fermion mass in the large- $d(R)$ limit. For related

QCD reviews on Dyson-Schwinger equations, we refer the reader to Refs. [106–109].

Starting from the partially bosonized action given in Eq. (23), we can derive the gap equation for the vacuum expectation value $\bar{\Phi}_0 = (\langle\sigma\rangle, \vec{0})$ of the scalar fields and the fermion mass, respectively. To this end, we first consider the so-called classical action $S \simeq \Gamma_{k \rightarrow \Lambda}$ which appears in the functional integral. Since the fermions appear only as bilinears in the action S , these fields can be integrated out straightforwardly. From the resulting expression, we obtain the (fully) bosonized effective action $\Gamma_B[\sigma, \vec{\pi}]$, which is a highly non-local object. From the stationary condition,

$$\left. \frac{\delta \Gamma_B[\sigma, \vec{\pi}]}{\delta \sigma} \right|_{\bar{\Phi}_0} = 0, \quad (36)$$

we then find the gap equation for $\langle\sigma\rangle$:¹²

$$1 = 8 \left(\frac{\bar{h}_\Lambda^2}{\bar{m}_\Lambda^2} \right) \text{Tr} \int \frac{d^3 p}{(2\pi)^3} \left[G_\psi^{(n)}(\vec{p}^2, \bar{g}\langle A_0 \rangle, \langle\sigma\rangle) - G_\psi^{(n)}(\Lambda^2, \bar{g}\langle A_0 \rangle, \langle\sigma\rangle) \right] \theta(\Lambda^2 - \vec{p}^2), \quad (37)$$

where

$$G_\psi^{(n)}(\vec{p}^2, \bar{g}\langle A_0 \rangle, \langle\sigma\rangle) = \frac{1}{(\nu_n + \bar{g}\langle A_0 \rangle)^2 + \vec{p}^2 + \bar{h}^2 \langle\sigma\rangle^2} \quad (38)$$

and $\nu_n = (2n+1)\pi T$. The trace Tr is defined as follows:

$$\text{Tr} \cdots = \text{tr}_R T \sum_{n=-\infty}^{\infty} \cdots \quad (39)$$

In Eq. (37) we have dropped the trivial solution $\langle\sigma\rangle = 0$. The integral on the right-hand side of the gap equation represents a Feynman integral with two internal fermion lines and two (Yukawa) vertices. In order to regularize this integral, we have employed a regularization scheme¹³ which corresponds to the one used to derive the RG flow equation for the four-fermion coupling $\bar{\lambda}_\psi$ in the previous section, see Eq. (25). The structure of the loop integral in the gap equation and on the right-hand side of the flow equation (25) is indeed identical.¹⁴ However, the prefactor on the right-hand side of the gap equation is only correct in leading order in the large- $d(R)$ expansion, in contrast to the associated prefactor in the flow equation (25) of the four-fermion coupling.¹⁵ Our general arguments concerning the relation of the chiral and the deconfinement phase transition in the previous section are not affected by this prefactor. The latter plays

only a qualitative, but no quantitative role. Therefore our findings concerning the interplay of the chiral and the deconfinement phase transition can be obtained from the gap equation (37) as well, as it should be. In fact, the fixed-points of the (dimensionless) four-fermion coupling can be viewed as critical values for the dimensionless quantity $\Lambda^2 \bar{h}_\Lambda^2 / \bar{m}_\Lambda^2$. This follows also from our discussion below Eq. (23). We refrain here from discussing this further. For a detailed discussion of fermionic RG flows and their relation to the gap equation, we refer the reader to, e. g., Ref. [27].

B. RG Flow at Large $d(R)$

Let us now discuss the fixed-point structure and the locking mechanism in the partially bosonized formulation of the matter sector, see Eq. (23). This formulation has the advantage that it allows us to systematically resolve the momentum dependence of the four-fermion interaction by means of a derivative expansion, see e. g. Ref. [27]. Eventually, this allows us to relate the initial value λ_ψ^{UV} of the four-fermion coupling to physical low-energy observables, such as meson masses and the pion decay constant f_π . The phase diagrams in the $(T, \lambda_\psi^{\text{UV}})$ plane can then be translated into phase diagrams in, e. g., the (T, f_π) plane. In other words, the partially bosonized formulation gives us access to the phase with broken chiral symmetry in the ground state.

From the effective action (23), we obtain the RG flow equations for the partially bosonized formulation. In leading order of an expansion in powers of $d(R)$, we find the following equations for the chirally symmetric regime:

$$\eta_\Phi = \frac{2}{3\pi^2} \sum_{l=1}^{d(R)} \mathcal{M}_{4,\pm}^{(F)}(\tau, 0, \nu_l |\phi|) h^2, \quad (40)$$

$$\eta_\psi = 0, \quad (41)$$

$$\partial_t h^2 = (2\eta_\psi + \eta_\Phi) h^2, \quad (42)$$

$$\partial_t m^2 = (\eta_\Phi - 2)m^2 + \frac{4}{\pi^2} \sum_{l=1}^{d(R)} l_1^{(F)}(\tau, 0, \nu_l |\phi|) h^2, \quad (43)$$

$$\partial_t \lambda_\Phi = 2\eta_\Phi \lambda_\Phi - \frac{8}{\pi^2} \sum_{l=1}^{d(R)} l_2^{(F)}(\tau, 0, \nu_l |\phi|) h^4, \quad (44)$$

where $\eta_\Phi = -\partial_t \ln Z_\Phi$, $\eta_\psi = -\partial_t \ln Z_\psi$, $h^2 = Z_\Phi^{-1} Z_\psi^{-2} \bar{h}^2$, $m^2 = k^{-2} Z_\Phi^{-1} \bar{m}^2$, and $\lambda_\Phi = Z_\Phi^{-2} \bar{\lambda}_\Phi$. The threshold functions can be found in App. A and Ref. [24]. We add that we do not distinguish between wave-function renormalizations longitudinal (Z_ψ^\parallel , Z_Φ^\parallel) and transversal (Z_ψ^\perp , Z_Φ^\perp) to the heat-bath. In the following we identify the corresponding wave-function renormalizations, $Z_\psi^\parallel = Z_\psi^\perp \equiv Z_\psi$ and $Z_\Phi^\parallel = Z_\Phi^\perp \equiv Z_\Phi$. In Ref. [100], it has indeed been found for the case $\langle A_0 \rangle = 0$ that the

¹² Here and in the following we assume that the ground state is homogeneous.

¹³ Often, a sharp cutoff is used to regularize the gap equation. In this case, the Λ -dependent term in the square brackets in Eq. (37) is absent, see Ref. [27].

¹⁴ Recall also that $\bar{h}_\Lambda^2 / \bar{m}_\Lambda^2$ can be identified with $\bar{\lambda}_\psi^{\text{UV}} \equiv \bar{\lambda}_{\psi,\Lambda}$.

¹⁵ Loosely speaking, the trace tr_R yields a factor of $d(R)$.

difference is small at low temperatures and only yields mild corrections to, e. g., the thermal masses close to and above the chiral phase transition. In our study of the partially bosonized formulation, we also include the RG flow of the four-boson coupling $\bar{\lambda}_\Phi$ associated with an additional term $\sim (\bar{\lambda}_\Phi/8)\bar{\Phi}^4$ in our ansatz (23). Since we have $\bar{\Phi} \sim (\bar{\psi}\mathcal{O}\psi)$, this type of interaction parametrizes higher-order fermionic self-interaction terms. These interactions are generated dynamically in the RG flow due to Yukawa-type quark-meson interactions. The initial value of the associated coupling is set to zero in our studies, i. e. $\bar{\lambda}_\Phi = 0$ at $k = \Lambda$. This allows us to map the partially bosonized theory onto our purely fermionic ansatz for the matter sector at the initial RG scale Λ .

In the large- $d(\text{R})$ limit, the flow of the four-boson coupling (and also of higher bosonic self-interactions $\sim \bar{\Phi}^{2n}$) does not contribute to the RG flows of Z_Φ , Z_ψ , h and m , at least in the chirally symmetric regime. This corresponds to the fact that the RG flow of the four-fermion coupling is decoupled from the RG flow of fermionic n -point functions of higher order, such as 8-fermion interactions.

Since we consider the large- $d(\text{R})$ limit in this subsection, we only have purely fermionic loops appearing on the right-hand side of the flow equations. We would like to stress that the large- $d(\text{R})$ expansion should not be confused with the widely used local potential approximation (LPA) where the running of the wave-function renormalizations is not taken into account.

Let us now relate the RG flow of the partially bosonized formulation to the RG flow of the purely fermionic formulation. Using Eq. (24) together with the flow equations (42) and (43), we recover the flow equation (25) of the four-fermion coupling λ_ψ in the large- $d(\text{R})$ limit, i. e.

$$\partial_t \left(\frac{h^2}{m^2} \right) \Big|_{d(\text{R}) \rightarrow \infty} \equiv \partial_t \lambda_\psi \Big|_{d(\text{R}) \rightarrow \infty}, \quad (45)$$

see also Eq. (63). Thus, only our choice for the ratio h^2/m^2 at the initial RG scale determines whether chiral symmetry is broken in the IR limit ($k \rightarrow 0$). Since the flow equation for the ratio h^2/m^2 is identical to the one for λ_ψ , we already anticipate that our statements concerning the temperature-order of the chiral and the deconfinement phase transition still hold in the partially bosonized formulation, see also Ref. [28].

After having shown the equivalence of the RG flow of h^2/m^2 and λ_ψ in the chirally symmetric regime, we now discuss the number of parameters in the matter sector of our model. Relation (45) seems to suggest that we only have one parameter, namely the ratio h^2/m^2 at the initial RG scale. Indeed, the value of the symmetry breaking scale k_{SB} depends only on our choice for h^2/m^2 at the initial RG scale. This suggests that a non-trivial IR repulsive fixed-point also exists in the plane spanned by the couplings h^2 and m^2 . From the above set of flow equations, however, we read off that

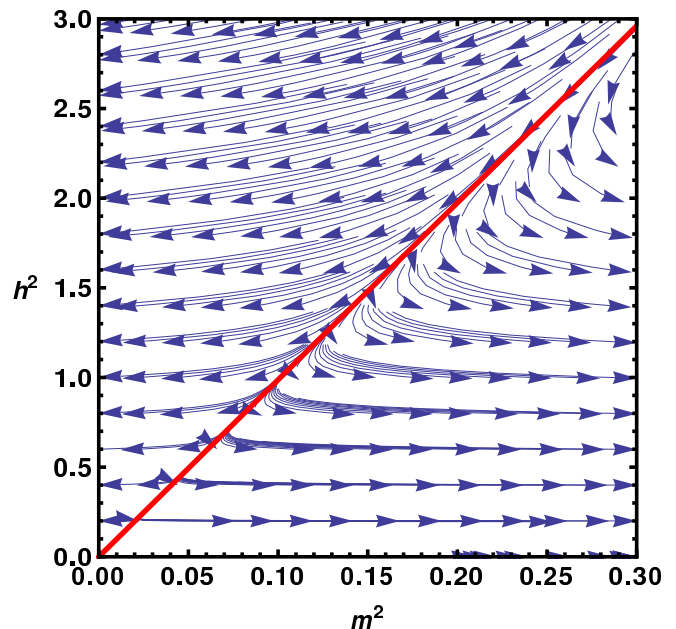


Figure 3. RG flow for fundamental fermions and $N = 3$ in leading order in the $1/d(\text{R})$ -expansion in the (h^2, m^2) -plane (at zero temperature). The red (solid) line represents the separatrix (critical manifold). The arrows indicate the direction of the RG flow towards the infrared, see text for an interpretation.

the system has only a Gaussian (non-interacting) fixed-point $(h_*^2, m_*^2)_{\text{Gau\ss}} = (0, 0)$, but no non-Gaussian fixed-point. This seems to be in contradiction to Eq. (45) and to our results from the purely fermionic formulation. Apart from the Gaussian fixed-point, we also observe that a separatrix exists in the plane spanned by h^2 and m^2 . The latter separates the (h^2, m^2) -plane into two disjunct regimes, see Fig. 3. In the large- $d(\text{R})$ limit, the functional form of the separatrix can be computed analytically. At $T = 0$, we find

$$h_{\text{sep.}}^2(m^2) = \frac{3\pi^2 m^2}{d(\text{R})} \equiv \lambda_{\psi, \infty}^* m^2, \quad (46)$$

where $\lambda_{\psi, \infty}^*$ is the value of the fixed point λ_ψ^* in the large- $d(\text{R})$ limit. Choosing initial conditions $(h_\Lambda^2, m_\Lambda^2)$ in the domain to the left of the separatrix, we find that the system flows into the regime with $m^2 < 0$, in which chiral symmetry is broken in the ground state. On the other hand, the system remains in the chirally symmetric regime, if we initialize the flow in the domain to the right of the separatrix, see Fig. 3. Loosely speaking, we have found that the separatrix takes over the role of the non-Gaussian fixed-point λ_ψ^* which is present in the point-like approximation of the purely fermionic formulation.

To further clarify the fate of the seemingly missing non-trivial fixed-point in the (h^2, m^2) -plane, we briefly consider the case $2 < d < 4$. In this case, a non-trivial fixed-point indeed exists in NJL-type and Gross-Neveu-type models, see e. g. Ref. [105]. This follows immediately

from a consideration of the RG flow of the dimensionless renormalized Yukawa coupling $h^2 = k^{d-4} Z_\Phi^{-1} Z_\psi^{-2} \bar{h}^2$:

$$\partial_t h^2 = (d - 4 + \eta_\Phi + 2\eta_\psi) h^2. \quad (47)$$

This differential equation has a Gaussian fixed-point and a non-Gaussian fixed-point h_*^2 for $2 < d < 4$ since $\eta_\Phi \sim h^2$ and $\eta_\Phi > 0$, see Refs. [105]. In the (h^2, m^2) -plane, we therefore have a non-trivial fixed-point with an IR attractive and IR repulsive direction for $2 < d < 4$. This non-trivial fixed-point represents the intersection point of two separatrices in the (h^2, m^2) -plane and corresponds to the non-trivial fixed-point of the associated four-fermion coupling. For $d \rightarrow 4$, this fixed-point then merges with the Gaussian fixed-point.

The non-existence of the non-Gaussian fixed-point in $d = 4$ implies that the Yukawa coupling h and the UV cutoff Λ should be considered as parameters of the theory, in addition to the ratio h_Λ^2/m_Λ^2 . In fact, for any finite UV cutoff, we can still define a critical value for the ratio $h^2/m^2 \sim \lambda_\psi$ above which spontaneous chiral symmetry breaking occurs in the long-range limit ($k \rightarrow 0$). However, since no non-trivial fixed-point with an IR attractive direction exists in the (h^2, m^2) -plane, the value of the Yukawa coupling at the symmetry breaking scale k_{SB} depends (strongly) on the initial conditions for the bosonic mass parameter and the Yukawa coupling itself. Once the system enters the regime with $m^2 < 0$, the RG flow of the Yukawa coupling effectively “freezes”. In this low-energy regime, the fermions acquire a mass and fermionic loops are therefore generically suppressed, see also discussion below. Hence we have three parameters in our simplified model ansatz for the matter sector, namely h_Λ^2/m_Λ^2 , h_Λ^2 and Λ . We would like to emphasize that there is indeed only a single parameter in $2 < d < 4$, as discussed in detail for the Gross-Neveu model in Ref. [105].

Let us now analyze the dynamics at finite T and $\langle A_0 \rangle$. Our discussion of Eq. (45) and of the RG flow in the (h^2, m^2) -plane at zero temperature already suggests that our general arguments concerning the relation of the deconfinement and the chiral phase transition in Sect. III are still valid. This is not too surprising: the point-like approximation in the purely fermionic formulation is a reasonable approximation in the chirally symmetric regime where the bosonic mass parameter m^2 is large over a wide range of scales and therefore suppresses the non-trivial momentum-dependence of the vertices.¹⁶ In any case, we now have to study the behavior of the separatrix in the (h^2, m^2) -plane for finite temperature T and finite $\langle A_0 \rangle$. To this end, we may even consider the dimensionless temperature $\tau = T/k$ as an additional coupling of the theory. Thus, the separatrix is no longer a

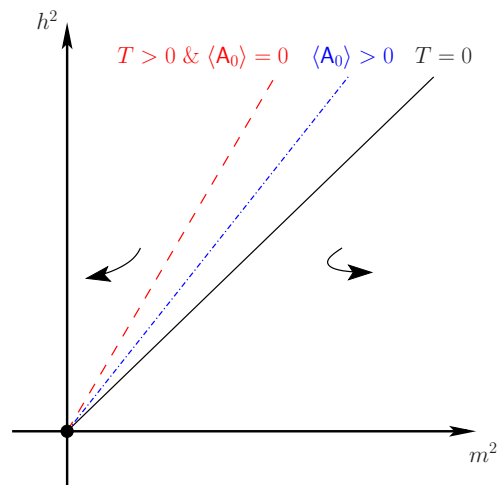


Figure 4. Sketch of the RG flow in leading order in the $1/d(\text{R})$ -expansion in the (h^2, m^2) -plane. The black dot denotes the Gaussian fixed-point. The separatrices are sketched for three different cases: vanishing temperature (black line), finite temperature and $\langle A_0 \rangle = 0$ (red/dashed line), and finite temperature and $\langle A_0 \rangle > 0$ (blue/dashed-dotted line). The dependence of the separatrices on the temperature and $\langle A_0 \rangle$ reflects the behavior of the non-Gaussian fixed-point of the four-fermion coupling, see Fig. 1. The arrows to the left and to the right of the separatrices indicate the direction of the RG flow towards the infrared, respectively.

one-dimensional manifold as it is the case at zero temperature. It rather represents a two-dimensional manifold. Again, the functional form of this critical manifold can be computed analytically. For $\tau = T/\Lambda \ll 1$, we find

$$h_{\text{sep.}}^2(m^2, \tau) = \frac{\lambda_{\psi, \infty}^* m^2}{1 - \pi^2 \mathcal{P}_R(T) \tau^2}, \quad (48)$$

where $\mathcal{P}_R(T)$ is defined in Eq. (35). We observe that the shape of the critical manifold depends on the temperature and the order parameter for center symmetry breaking, see Fig. 4.

The critical manifold allows us to define a necessary condition for chiral symmetry breaking at finite temperature. Solving Eq. (48) for τ , we obtain $\tau_{\text{sep.}}(m^2, h^2)$. Choosing now $\tau < \tau_{\text{sep.}}$ for a given set of initial values $(h_\Lambda^2, m_\Lambda^2)$, the theory necessarily approaches the regime with broken chiral symmetry in the IR limit. For $\tau > \tau_{\text{sep.}}$, on the other hand, the theory remains in the chirally symmetric regime. For a given value of the UV cutoff Λ and $(h_\Lambda^2, m_\Lambda^2)$, the quantity $\tau_{\text{sep.}}$ is therefore nothing but the dimensionless chiral phase transition temperature, $\tau_{\text{sep.}} = T_\chi/\Lambda$. In fact, $T_\chi = \Lambda \tau_{\text{sep.}}$ agrees with the result from Eq. (34). Thus, our general statements in Sect. III concerning the interplay of the chiral and the deconfinement phase transition still hold.

Let us now discuss how our phase diagrams in the $(T, \lambda_\psi^{\text{UV}})$ -plane can be translated into phase diagrams in, e. g., the (T, f_π) -plane. To this end, we need to follow the RG flow down to the long-range limit. As discussed

¹⁶ Recall that the bosons mediate the interaction between the fermions in the partially bosonized formulation. In this spirit, the boson propagators parametrize the momentum dependence of the four-fermion coupling, see e. g. Ref. [27] for a detailed discussion.

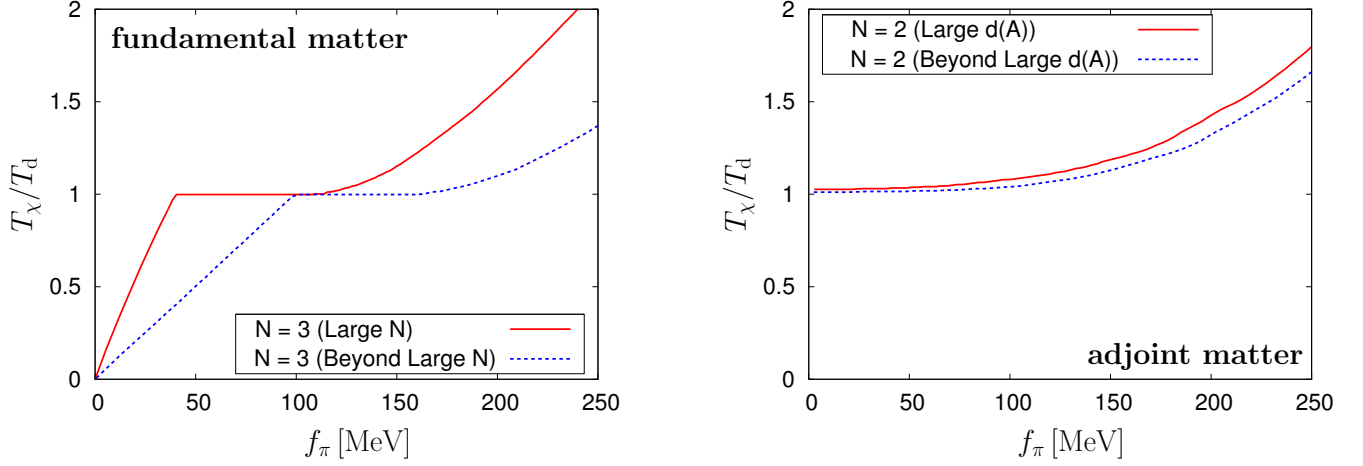


Figure 5. In the left panel, we show the phase diagram for two massless fundamental quarks and $N = 3$ in the plane spanned by the rescaled temperature T_χ/T_d and the value of the pion decay constant f_π at $T = 0$. In the right panel, the corresponding phase diagram for two massless quark flavors in the adjoint representation and $N = 2$ is shown. In both panels, the results from the large- $d(R)$ approximation are given by the red (solid) line, whereas the blue (dashed) line depicts the results from our study including corrections beyond the large- $d(R)$ limit.

in Sect. II B, the mass parameter m^2 assumes negative values in the regime with broken chiral symmetry in the ground state and the vacuum expectation value $\langle \Phi \rangle \equiv \bar{\Phi}_0$ becomes finite. It is therefore convenient to study the RG flow of $\bar{\Phi}_0$ and $\bar{\lambda}_\Phi$ rather than that of \bar{m}^2 and $\bar{\lambda}_\Phi$. The flow equation of $\bar{\Phi}_0$ can be obtained from the stationary condition:

$$\frac{d}{dt} \left[\frac{\partial}{\partial \bar{\Phi}^2} \left(\frac{1}{2} \bar{m}^2 \bar{\Phi}^2 + \frac{1}{8} \bar{\lambda}_\Phi \bar{\Phi}^4 \right) \right]_{\bar{\Phi}_0} \stackrel{!}{=} 0. \quad (49)$$

To be specific, we find the following RG flow equations for the regime with broken chiral symmetry in the ground state:

$$\eta_\Phi = \frac{2}{3\pi^2} \sum_{l=1}^{d(R)} \mathcal{M}_{4,l}^{(F)}(\tau, m_q^2, \nu_l |\phi|) h^2, \quad (50)$$

$$\eta_\psi = 0, \quad (51)$$

$$\partial_t h^2 = (2\eta_\psi + \eta_\Phi) h^2, \quad (52)$$

$$\begin{aligned} \partial_t \bar{\Phi}_0^2 &= -(\eta_\Phi + 2) \bar{\Phi}_0^2 \\ &\quad - \frac{8}{\pi^2} \sum_{l=1}^{d(R)} l_1^{(F)}(\tau, m_q^2, \nu_l |\phi|) \frac{h^2}{\lambda_\Phi}, \end{aligned} \quad (53)$$

$$\partial_t \lambda_\Phi = 2\eta_\Phi \lambda_\Phi - \frac{8}{\pi^2} \sum_{l=1}^{d(R)} l_2^{(F)}(\tau, m_q^2, \nu_l |\phi|) h^4, \quad (54)$$

where $\bar{\Phi}_0^2 = k^{-2} Z_\Phi \bar{\Phi}_0^2$ and the (dimensionless) renormalized constituent quark mass reads

$$m_q^2 = h^2 \bar{\Phi}_0^2.$$

In the following we will identify the pion decay constant f_π with $Z_\Phi^{1/2} \bar{\Phi}_0$. The (dimensionless) renormalized meson masses are given by

$$m_\pi^2 = 0 \quad \text{and} \quad m_\sigma^2 = \lambda_\Phi \bar{\Phi}_0^2.$$

Since we are working in the large- $d(R)$ limit in this section, the latter do not appear explicitly on the right side of the flow equations.

Recall that the scale for m_q and m_σ is set by the symmetry breaking scale k_{SB} which is set by our choice for h_Λ^2/m_Λ^2 . The role of the Yukawa coupling (as an additional parameter) becomes now apparent from the relation

$$m_\sigma^2 = \lambda_\Phi \bar{\Phi}_0^2 \sim h^4 \bar{\Phi}_0^2 \sim h^2 m_q^2,$$

which follows from the flow equations of the couplings. Since the flow of the Yukawa coupling is not governed by the presence of a non-trivial IR attractive fixed-point, its value depends on k_{SB} and the initial value h_Λ , as discussed above. Therefore the ratio m_σ^2/m_q^2 depends on our choice for h_Λ . On the other hand, the initial value of the coupling λ_Φ does not represent a free parameter of the theory. It is set to zero at $k = \Lambda$ and therefore generated dynamically in the RG flow, see also Eq. (23).

Using the flow equations (40)-(44) and (50)-(54), we can now proceed and compute the phase diagram in the plane spanned by the temperature and the value of the pion decay constant at $T = 0$. In Fig. 5 (left panel) we show our results for quarks in the fundamental representation and $N = 3$. For adjoint matter and $N = 2$, our results can be found in the right panel of Fig. 5. To obtain these results, we have used $\Lambda = 1 \text{ GeV}$. Moreover, we have again employed the data for the ground-state values of $\langle A_0 \rangle$ as obtained from a RG study of $\text{SU}(N)$ Yang-Mills theories [33, 70].

In the case of fundamental matter and $N = 3$, we observe that the upper end of the locking window ($T_d \approx T_\chi$) roughly coincides with the physical value of the pion decay constant, provided that we fix the initial condition of the Yukawa coupling such that $m_q \approx 300 \text{ MeV}$

for $f_\pi \approx 90$ MeV, see left panel of Fig. 5. This observation is in accordance with results from lattice simulations and general expectations. For $f_\pi \lesssim 30$ MeV, we find $T_\chi < T_d$. More precisely, we observe that $T_\chi \sim f_\pi$ for small values of f_π . For $f_\pi \gtrsim 100$ MeV ($m_q \gtrsim 350$ MeV), we then have $T_\chi > T_d$. In this regime, the quarks are very heavy and the two phase transitions are disentangled. Concerning the role of the Yukawa coupling, we find that the lower end of the locking window is shifted to smaller values of f_π when we increase the initial value of the Yukawa coupling. Moreover, we find that the size of the window does not strongly depend on our choice for h_Λ . This is not unexpected since we have found in our analysis of the fermionic fixed-point structure that the size of the locking window is solely related to the value of the ratio $h_\Lambda^2/m_\Lambda^2 = \lambda_\psi^{\text{UV}}$. However, the translation of the upper and lower end of the locking window in λ_ψ^{UV} -space into values of physical observables does indeed depend on our choice for both h_Λ as well as h_Λ^2/m_Λ^2 , as discussed above.

For adjoint matter and $N = 2$ as well as $N = 3$, we find that $T_\chi > T_d$, even for very small values of f_π . We refer to Fig. 5 for our results for $N = 2$. To obtain these results, we have used $h_\Lambda = 3$. However, $T_\chi > T_d$ holds for arbitrary values of h_Λ in the large $d(\text{R})$ limit, as suggested by our fermionic fixed-point analysis. In fact, our results in the large- $d(\text{R})$ limit are in accordance with our results in Fig. 2, as it should be. For increasing f_π , we observe that the chiral phase transition temperature increases further. Thus, we have $T_\chi > T_d$ for all values of f_π .

Finally we would like to add that it is also possible to tune the parameters h_Λ^2/m_Λ^2 and m_Λ^2 such that we obtain $T_\chi/T_d \approx 7.8$ for $N = 3$, as found in lattice simulations [50] of adjoint QCD without λ_ψ -deformation. Of course, this requires that the UV cutoff Λ is adjusted to larger values in order to ensure that T/Λ is sufficiently small for the temperature range under consideration, see Ref. [52] for a PNJL model study in a mean-field approximation.

C. RG Flow Beyond the Large- $d(\text{R})$ Approximation

In the following we study the robustness of our results of the previous sections with respect to $1/d(\text{R})$ -corrections. This includes an analysis of the role of Goldstone-mode fluctuations which are absent in the large- $d(\text{R})$ limit.

Our RG approach allows us to systematically include $1/d(\text{R})$ -corrections. Due to the one-loop structure of the Wetterich equation, these corrections correspond to 1PI diagrams with at least one internal boson line. In the chirally symmetric regime ($\Phi_0 \equiv 0$), we then find the following set of equations:

$$\eta_\Phi = \frac{2}{3\pi^2} \sum_{l=1}^{d(\text{R})} \mathcal{M}_{4,1}^{(\text{F})}(\tau, 0, \nu_l|\phi|) h^2, \quad (55)$$

$$\begin{aligned} \partial_t h^2 &= (2\eta_\psi + \eta_\Phi) h^2 \\ &\quad - \frac{2}{\pi^2} \frac{1}{d(\text{R})} \sum_{l=1}^{d(\text{R})} l_{1,1}^{(\text{FB})}(\tau, 0, \nu_l|\phi|, m^2) h^4, \end{aligned} \quad (56)$$

$$\begin{aligned} \partial_t m^2 &= (\eta_\Phi - 2)m^2 - \frac{3}{2\pi^2} l_1(\tau, m^2) \lambda_\Phi \\ &\quad + \frac{4}{\pi^2} \sum_{l=1}^{d(\text{R})} l_1^{(\text{F})}(\tau, 0, \nu_l|\phi|) h^2, \end{aligned} \quad (57)$$

$$\begin{aligned} \partial_t \lambda_\Phi &= 2\eta_\Phi \lambda_\Phi + \frac{3}{\pi^2} l_2(\tau, m^2) \lambda_\Phi^2 \\ &\quad - \frac{8}{\pi^2} \sum_{l=1}^{d(\text{R})} l_2^{(\text{F})}(\tau, 0, \nu_l|\phi|) h^4, \end{aligned} \quad (58)$$

In regime with broken chiral symmetry ($\Phi_0 \neq 0$), the flow of the couplings is determined by the following equations:¹⁷

$$\eta_\Phi = \frac{2}{3\pi^2} \sum_{l=1}^{d(\text{R})} \mathcal{M}_{4,1}^{(\text{F})}(\tau, m_q^2, \nu_l|\phi|) h^2, \quad (59)$$

$$\begin{aligned} \partial_t h^2 &= (2\eta_\psi + \eta_\Phi) h^2 \\ &\quad - \frac{1}{\pi^2} \frac{1}{d(\text{R})} \sum_{l=1}^{d(\text{R})} \left[3l_{1,1}^{(\text{FB})}(\tau, m_q^2, \nu_l|\phi|, m_\pi^2) \right. \\ &\quad \left. - l_{1,1}^{(\text{FB})}(\tau, m_q^2, \nu_l|\phi|, m_\sigma^2) \right] h^4, \end{aligned} \quad (60)$$

$$\begin{aligned} \partial_t \Phi_0^2 &= -(\eta_\Phi + 2)\Phi_0^2 + \frac{3}{2\pi^2} l_1(\tau, m_\sigma^2) + \frac{3}{2\pi^2} l_1(\tau, m_\pi^2) \\ &\quad - \frac{8}{\pi^2} \sum_{l=1}^{d(\text{R})} l_1^{(\text{F})}(\tau, m_q^2, \nu_l|\phi|) \frac{h^2}{\lambda_\Phi}, \end{aligned} \quad (61)$$

$$\begin{aligned} \partial_t \lambda_\Phi &= 2\eta_\Phi \lambda_\Phi + \frac{9}{4\pi^2} l_2(\tau, m_\sigma^2) \lambda_\Phi^2 + \frac{3}{4\pi^2} l_2(\tau, m_\pi^2) \lambda_\Phi^2 \\ &\quad - \frac{8}{\pi^2} \sum_{l=1}^{d(\text{R})} l_2^{(\text{F})}(\tau, m_q^2, \nu_l|\phi|) h^4. \end{aligned} \quad (62)$$

The threshold functions¹⁸ can be found in App. A and Ref. [24]. For simplicity, we do not include the running of the fermionic wave-function renormalization in the present study, although it can be taken into account straightforwardly, as illustrated in, e. g., Refs. [20, 24, 99, 100] for the case $\langle A_0 \rangle = 0$. As discussed in the previous subsection, this is *not* an approximation in the large- $d(\text{R})$

¹⁷ In the flow equations for the Yukawa coupling and the bosonic wave-function renormalization, we have dropped terms proportional to Φ_0 . Concerning the Yukawa coupling, it has been found that these terms only yield mild (quantitative) corrections [20, 110, 111]. With regard to the bosonic wave-function renormalization, these terms are of crucial importance for an accurate computation of the critical exponents [99, 112] which is beyond the scope of the present work.

¹⁸ Note that the functions $l_1^{(\text{B})}$, $l_2^{(\text{B})}$ and $l_{1,1}^{(\text{FB})}$ depend implicitly on η_Φ .

limit. Beyond the large- $d(\text{R})$ limit, it has been found in Refs. [20, 24, 99, 100] that the anomalous dimension η_ψ is still small. This can be traced back to the fact that the running of Z_Φ is solely governed by 1PI diagrams with at least one internal boson and fermion line. Such diagrams are parametrically suppressed in the regime with broken chiral symmetry due to the large mass of the fermions, but they are also suppressed in the chirally symmetric regime due to the large mass of the bosons. As a consequence, the running of Z_ψ only yields mild corrections to the symmetry breaking scale k_{SB} . In the following we will only take into account $1/d(\text{R})$ -corrections in those RG equations which are also non-zero in the large- $d(\text{R})$ limit. The inclusion of the running of Z_ψ is left to future work.

Using the flow equations of the Yukawa coupling and the bosonic mass parameter in the chirally symmetric regime, we can study again the RG flow of the ratio h^2/m^2 . We now find

$$\begin{aligned} \partial_t \left(\frac{h^2}{m^2} \right) &= (2+2\eta_\psi) \left(\frac{h^2}{m^2} \right) + \frac{3}{2\pi^2} l_1(\tau, m^2) \lambda_\Phi \left(\frac{h^2}{m^4} \right) \\ &\quad - \frac{4}{\pi^2} \sum_{l=1}^{d(\text{R})} l_1^{(\text{F})}(\tau, m_q^2, \nu_l|\phi) \left(\frac{h^2}{m^2} \right)^2 \\ &\quad - \frac{2}{\pi^2} \frac{1}{d(\text{R})} \sum_{l=1}^{d(\text{R})} l_{1,1}^{(\text{FB})}(\tau, m_q^2, \nu_l|\phi, m^2) \left(\frac{h^4}{m^2} \right). \quad (63) \end{aligned}$$

Using $\lambda_\psi \equiv (h^2/m^2)$, the first term on the right-hand side as well as the terms in the second line can be straightforwardly identified with terms appearing in the RG equation of the four-fermion coupling λ_ψ , see Eq. (25). These are the leading order terms of the large- $d(\text{R})$ expansion. The second term on the right-hand side corresponds to a $1/d(\text{R})$ -correction and effectively couples the flow of h^2/m^2 (\sim four-fermion coupling) to the flow of the four-boson coupling (\sim 8-fermion coupling). Since it can be shown that the RG flow of fermionic self-interactions is fully decoupled in the point-like limit [27], this term resolves (part of) the momentum dependence of the four-fermion interaction. The expression in the third line also represents a $1/d(\text{R})$ -correction and can be traced back to the running of the Yukawa coupling. Without the terms in the third line, it is not possible to reproduce the prefactor of the term $\sim \lambda_\psi^2$ in the flow equation (25) in the limit $m^2 \gg 1$ (point-like limit). As pointed out in Ref. [28], this can be seen immediately from the following relation

$$l_{1,1}^{(\text{FB})}(\tau, m_q^2, \nu_l|\phi, m^2) \xrightarrow{(m \gg 1)} \frac{1}{m^2} l_1^{(\text{F})}(\tau, m_q^2, \nu_l|\phi).$$

For finite m^2 , the expression in the third line on the right-hand side of Eq. (63) also resolves part of the momentum structure of the four-fermion vertex beyond the point-like limit.

Let us now discuss our results for the phase diagrams in the (T, f_π) -plane beyond the large- $d(\text{R})$ limit. In Fig. 5, we show our results for quarks in the fundamental representation and $N = 3$ as well as for quarks in the adjoint

representation and $N = 2$. We have chosen these representations and values for N since they play a prominent role from a phenomenological point of view. For quarks in the fundamental representation, we observe that our results agree with those from our large- N study, at least on a qualitative level.¹⁹ This means we still have three distinct regimes: one regime with $T_\chi < T_d$ for small values of f_π , one regime with $T_\chi \approx T_d$ (locking window), and a regime with $T_\chi > T_d$ for large values of f_π . Also, the size of the locking window is roughly the same as in the large- N approximation. However, the lower and the upper end of the window have been shifted to larger values of f_π . The locking window begins at $f_\pi \approx 100$ MeV and ends at $f_\pi \approx 150$ MeV. Thus, the physical value of the pion decay constant is slightly below the lower end of the locking window.

For quarks in the adjoint representation and $N = 2$, we find that our results are less strongly affected by corrections arising beyond the large- $d(\text{A})$ approximation, see Fig. 5 (right panel). To be specific, we observe that $T_\chi > T_d$ for $f_\pi > 0$, even if we take $1/d(\text{R})$ -corrections into account. The results only differ with respect to the slope of the chiral phase transition temperature as a function of f_π . As in the case of fermions in the fundamental representation, the slope is steeper in the large- $d(\text{A})$ limit. We conclude that fluctuations of the Nambu-Goldstone modes tend to lower the sensitivity of T_χ on f_π .

The results for adjoint quarks in Fig. 5 have been obtained by choosing $h_\Lambda = 3$ for the initial value of the Yukawa coupling. The value of the pion decay constant can then be varied by varying only the initial value of the bosonic mass parameter m_Λ . As in the case of fundamental quarks, it is in principle possible to fix the initial condition for the Yukawa coupling by requiring that the constituent quark mass assumes a given value for a given value of the pion decay constant. For adjoint quarks, we refrain from fixing the initial condition h_Λ in this way but rather illustrate how our results depend on the choice for h_Λ , see Fig. 6. We observe that the dependence of T_χ on f_π becomes stronger for larger values of h_Λ . Most importantly, however, we find that $T_\chi > T_d$ for $N = 2$, independent of our choice for $h_\Lambda > 0$. We stress that the mechanism underlying this observation is the deformation of the (fermionic) fixed-point structure due to the presence of the confining gauge dynamics.

Let us finally comment on the order of the chiral phase transition in the (T, f_π) phase diagram. In Ref. [28], it was found for fundamental fermions and $N = 3$ that the

¹⁹ Note that we have fixed the initial value of the Yukawa coupling by requiring that $m_q \approx 300$ MeV for $f_\pi \approx 90$ MeV. The same initial value for the Yukawa coupling has then been used to compute the phase transition temperature for all other values of f_π as well. Thus, we have only varied the initial value of the bosonic mass parameter m^2 to change the value of f_π . Recall that $\lambda_\psi \sim h^2/m^2$.

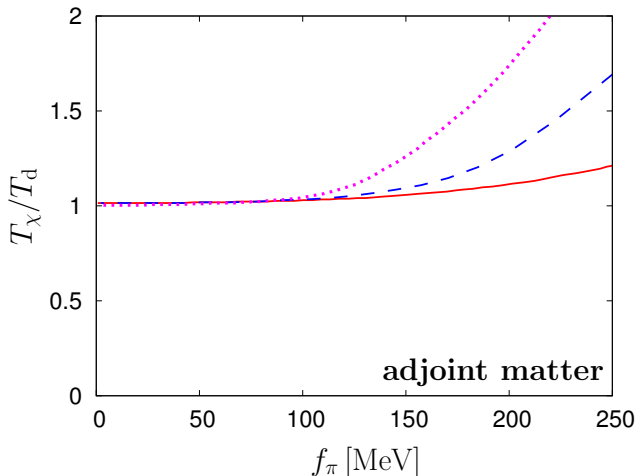


Figure 6. Ratio T_χ/T_d of the chiral and the deconfinement phase transition temperature as a function of the zero-temperature value of the pion decay constant f_π for two massless adjoint quarks and $N = 2$. The various lines illustrate the dependence of our results on the initial condition (UV value) for the Yukawa coupling. The results have been obtained for $h_\Lambda = 2, 3, 4$ (from bottom to top).

chiral phase transition is of first order within the locking window. To be more precise, we observe that the chiral phase transition is of first order for $100 \text{ MeV} \lesssim f_\pi \lesssim 150 \text{ MeV}$ for $N = 3$. Above and below the locking window, the chiral phase transition is of second order. In particular, the observation of a first-order region might be a shortcoming of our approximations: we have simply used the data for $\langle A_0 \rangle(T)$ from a study of pure $SU(3)$ Yang-Mills theory, but neglected the back-reaction of the matter sector on the confinement order parameter. Within the locking window, the first-order phase transition in the gauge sector induces a first-order chiral phase transition. As argued in Ref. [28], a first-order chiral transition may still occur in the (T, f_π) -plane, even if we go beyond the present approximation. However, this would then require that the confinement order parameter rises rapidly for $T \gtrsim T_d$. A test of this conjecture is beyond the scope of the present work and left to future studies.

For adjoint matter and $N = 2$, we observe that $T_\chi > T_d$ for all values of $f_\pi > 0$. Therefore the dynamics at the chiral phase transition is less affected by the confining dynamics. Loosely speaking, the latter only pushes T_χ above T_d . Within the present approximation, we therefore find that the chiral phase transition is of second order for all values of $f_\pi > 0$. This result is consistent with lattice simulations for $N = 2$, see Refs. [49, 50].

V. CONCLUSIONS AND OUTLOOK

In the present paper we have analyzed the interplay of the chiral and the deconfinement phase transition in

gauge theories with matter fields in different representations, with an emphasis on quarks in the fundamental and the adjoint representation. To this end, we have computed phase diagrams in the plane spanned by the temperature and the pion decay constant using a simple ansatz for the quantum effective action. This ansatz allowed us to study the fixed-point structure in the matter sector analytically. In particular, it opened up the possibility to analyze the impact of the confinement order parameter on the chiral fixed-point structure. The latter is directly related to the order parameter for chiral symmetry breaking.

For theories with quark fields living in a given representation R , we have found that the interplay of the chiral and the deconfinement phase transition clearly depends on the sign of the quantity $\text{tr}_R L_R[\langle A_0 \rangle]$ in the center symmetric phase. The relation of $\text{tr}_R L_R[\langle A_0 \rangle]$ to the standard Polyakov loop (for a given representation R) has been discussed in detail in Sect. II A. To be specific, our fixed-point analysis suggests that $T_\chi > T_d$ for adjoint quarks, at least in the large- $d(R)$ limit. This observation is in accordance with results from lattice simulations [49–51]. For quarks in the fundamental representation, our findings are also compatible with lattice QCD studies [8–10, 13], first-principles continuum studies [12, 15, 113], and earlier analytic (model) studies [1, 28, 102].

We have also investigated how robust our predictions for the (T, f_π) phase diagram are, once $1/d(R)$ -corrections are taken into account in the matter sector. Such corrections are associated with fluctuations of the Nambu-Goldstone modes of the theory. For quarks in the fundamental representation, we have found that the locking window ($T_\chi \approx T_d$) is shifted to larger values of f_π but remains finite. At the physical point ($f_\pi \approx 90 \text{ MeV}$), we have $T_\chi \lesssim T_d$. For adjoint quarks and $N = 2$, we have found that $T_\chi > T_d$ for all values of $f_\pi > 0$, even if $1/d(R)$ -corrections are taken into account. In this respect, the finite-temperature dynamics of gauge theories with adjoint matter appear to be distinct from gauge theories with fundamental matter, at least for $N = 2$. Recall that this observation is also consistent with lattice studies of $SU(2)$ gauge theory with two flavors of adjoint quarks [49–51].

We would like to add that our fixed-point analysis can also help to guide the development of QCD low-energy models in the future. To be specific, we have used the order-parameter potential spanned by the background temporal gauge field. Moreover, we have not employed the assumption $\text{tr}_R L_R[\langle A_0 \rangle] = \langle \text{tr}_R L_R[A_0] \rangle$ which is often used in PNJL/PQM-type model studies. Instead, we have considered the quantity $\text{tr}_R L_R[\langle A_0 \rangle]$ in the present study. This corresponds to working in a specific class of gauges, namely the class of Polyakov-DeWitt gauges. Our study suggests that the assumption $\text{tr}_R L_R[\langle A_0 \rangle] = \langle \text{tr}_R L_R[A_0] \rangle$ is justified in a mean-field approximation ($N \rightarrow \infty$). For finite N (and, in particular, for quarks in representations other than the fundamental one), however, the situation may change. De-

pending on the representation R , the sign of $\text{tr}_R L_R[\langle A_0 \rangle]$ can be different below and above the phase transition, whereas $\langle \text{tr}_R L_R[A_0] \rangle$ can be defined to be positive for all temperatures.

Of course, the present analysis can be improved in many ways. For example, one may consider to take into account the back-reaction of the matter fields on the quantity $\text{tr}_R L_R[\langle A_0 \rangle]$. Such contributions will push $\text{tr}_R L_R[\langle A_0 \rangle]$ to larger values in the low-temperature phase. We expect that this will weaken the mechanisms governing the dynamics in our present study. For fundamental quarks, for example, this may shrink the locking window. For adjoint quarks, on the other hand, the quantity $\text{tr}_R L_R[\langle A_0 \rangle]$ may still be negative over a wide range of temperatures. Therefore, $T_\chi > T_d$ may persist for $N = 2$, even if we take these back-reactions into account. In any case, we have presented first predictions for the (T, f_π) phase diagram and our analysis reveals a simple mechanism governing the interplay of the chiral and the deconfinement phase transition. It would be interesting to see whether and how this mechanism persists in the presence of a finite quark chemical potential and/or a finite external magnetic field. The latter deforms the fermionic fixed-point structure in a way [103, 104] which is indeed reminiscent of the deformation discussed here for adjoint quarks.

Acknowledgments. The authors are very grateful to H. Gies, J. M. Pawłowski and B.-J. Schaefer for useful discussions and critical comments on the manuscript. Moreover, the authors thank R. Alkofer, A. Janot, D. D. Scherer and A. Wipf for useful discussions. JB acknowledges support by the DFG research training group GRK 1523/1, and by the Helmholtz International Center for FAIR within the LOEWE program of the State of Hesse. TKH is recipient of a DOC-fORTE-fellowship of the Austrian Academy of Sciences and supported by the FWF doctoral program DK-W1203-N16.

Appendix A: Threshold functions

In the computation of the RG flow equations, a regulator function needs to be specified which determines the regularization scheme [82]. Here, we have used a linear spatial regulator function for the bosonic as well as for the fermionic degrees of freedom [114–118]. To be

specific, we have chosen

$$R_B(\vec{p}^2) = \vec{p}^2 \left(\frac{k^2}{\vec{p}^2} - 1 \right) \theta(k^2 - \vec{p}^2) \equiv \vec{p}^2 r_B \left(\frac{\vec{p}^2}{k^2} \right), \quad (\text{A1})$$

for the bosons, whereas we have chosen

$$R_\psi(\vec{p}) = \vec{p} \left(\sqrt{\frac{k^2}{\vec{p}^2}} - 1 \right) \theta(k^2 - \vec{p}^2) \equiv \vec{p} r_\psi \left(\frac{\vec{p}^2}{k^2} \right) \quad (\text{A2})$$

for the fermionic degrees of freedom.

Now we define the threshold function $\mathcal{M}_{4,\perp}^{(F)}$. This function represents a 1PI diagram with two internal fermion lines and contributes to the RG flow of the bosonic wavefunction renormalization. Those threshold functions, which are not defined in this appendix, can be found in Refs. [24, 27, 28].

To define the threshold function $\mathcal{M}_{4,\perp}^{(F)}$, it is convenient to introduce a dimensionless propagator for the fermions:

$$\tilde{G}_\psi(x_0, \omega) = \frac{1}{x_0 + x(1 + r_\psi)^2 + \omega}, \quad (\text{A3})$$

where $x = \vec{p}^2/k^2$. In terms of this propagator, the threshold function entering the anomalous dimension of the bosons can be written as follows:

$$\begin{aligned} & \mathcal{M}_{4,\perp}^{(F)}(\tau, \omega, \mu) \\ &= (d-1)\tau \sum_{n=-\infty}^{\infty} \int_0^\infty dx x^{\frac{d-3}{2}} \tilde{\partial}_t \left\{ x(1+r_\psi) \tilde{G}_\psi(x_0^\psi, \omega) \times \right. \\ & \quad \times \left[\frac{2x}{d-1} \left(\frac{d^2}{dx^2} (1+r_\psi) \tilde{G}_\psi(x_0^\psi, \omega) \right) \right. \\ & \quad \left. \left. + \frac{d+1}{d-1} \left(\frac{d}{dx} (1+r_\psi) \tilde{G}_\psi(x_0^\psi, \omega) \right) \right] \right. \\ & \quad \left. + x_0^\psi \tilde{G}_\psi(x_0^\psi, \omega) \left[\frac{2x}{d-1} \left(\frac{d^2}{dx^2} \tilde{G}_\psi(x_0^\psi, \omega) \right) \right. \right. \\ & \quad \left. \left. + \left(\frac{d}{dx} \tilde{G}_\psi(x_0^\psi, \omega) \right) \right] \right\}, \quad (\text{A4}) \end{aligned}$$

where $x_0^\psi = (\tilde{\nu}_n + 2\pi\tau\mu)^2$ and $\tilde{\nu}_n = (2n+1)\pi\tau$. Here, the derivative $\tilde{\partial}_t$ with respect to the regulator function is defined as follows:

$$\tilde{\partial}_t = \frac{1}{x^{1/2}} \theta(1-x) \frac{\partial}{\partial r_\psi}. \quad (\text{A5})$$

We do not display terms $\propto \eta_\psi$ since we have not taken into account these contributions in our numerical analysis.

[1] P. N. Meisinger and M. C. Ogilvie, Phys. Lett. **B379**, 163 (1996), hep-lat/9512011.

[2] F. Karsch, E. Laermann, and A. Peikert, Nucl. Phys. **B605**, 579 (2001), hep-lat/0012023.

- [3] F. Karsch and E. Laermann, hep-lat/0305025.
- [4] A. Mocsy, F. Sannino, and K. Tuominen, Phys. Rev. Lett. **92**, 182302 (2004), hep-ph/0308135.
- [5] K. Fukushima, Phys. Lett. **B591**, 277 (2004), hep-ph/0310121.
- [6] E. Megias, E. Ruiz Arriola, and L. L. Salcedo, Phys. Rev. **D74**, 065005 (2006), hep-ph/0412308.
- [7] C. Ratti, M. A. Thaler, and W. Weise, Phys. Rev. **D73**, 014019 (2006), hep-ph/0506234.
- [8] M. Cheng *et al.*, Phys. Rev. **D74**, 054507 (2006), hep-lat/0608013.
- [9] Y. Aoki, Z. Fodor, S. D. Katz, and K. K. Szabo, Phys. Lett. **B643**, 46 (2006), hep-lat/0609068.
- [10] Y. Aoki, G. Endrodi, Z. Fodor, S. D. Katz, and K. K. Szabo, Nature **443**, 675 (2006), hep-lat/0611014.
- [11] B.-J. Schaefer, J. M. Pawłowski, and J. Wambach, Phys. Rev. **D76**, 074023 (2007), 0704.3234.
- [12] J. Braun, L. M. Haas, F. Marhauser, and J. M. Pawłowski, Phys. Rev. Lett. **106**, 022002 (2011), 0908.0008.
- [13] Y. Aoki *et al.*, JHEP **06**, 088 (2009), 0903.4155.
- [14] T. K. Herbst, J. M. Pawłowski, and B.-J. Schaefer, Phys. Lett. **B696**, 58 (2011), 1008.0081.
- [15] J. M. Pawłowski, AIP Conf. Proc. **1343**, 75 (2011), 1012.5075.
- [16] T. K. Herbst, J. M. Pawłowski, and B.-J. Schaefer, (2012), 1202.0758.
- [17] P. Braun-Munzinger, K. Redlich, and J. Stachel, (2003), nucl-th/0304013.
- [18] Y. Nambu and G. Jona-Lasinio, Phys. Rev. **122**, 345 (1961).
- [19] Y. Nambu and G. Jona-Lasinio, Phys. Rev. **124**, 246 (1961).
- [20] H. Gies and C. Wetterich, Phys. Rev. **D69**, 025001 (2004), hep-th/0209183.
- [21] H. Gies and J. Jaeckel, Eur. Phys. J. **C46**, 433 (2006), hep-ph/0507171.
- [22] J. Braun and H. Gies, Phys. Lett. **B645**, 53 (2007), hep-ph/0512085.
- [23] J. Braun and H. Gies, JHEP **06**, 024 (2006), hep-ph/0602226.
- [24] J. Braun, Eur. Phys. J. **C64**, 459 (2009), 0810.1727.
- [25] J. Braun and H. Gies, JHEP **05**, 060 (2010), 0912.4168.
- [26] J. Braun, C. S. Fischer, and H. Gies, Phys. Rev. **D84**, 034045 (2011), 1012.4279.
- [27] J. Braun, J. Phys. **G39**, 033001 (2012), 1108.4449.
- [28] J. Braun and A. Janot, Phys. Rev. **D84**, 114022 (2011), 1102.4841.
- [29] L. McLerran and R. D. Pisarski, Nucl. Phys. **A796**, 83 (2007), 0706.2191.
- [30] F. R. Brown *et al.*, Phys. Rev. Lett. **65**, 2491 (1990).
- [31] B.-J. Schaefer and M. Wagner, Phys. Rev. **D79**, 014018 (2009), 0808.1491.
- [32] M. Panero, Phys. Rev. Lett. **103**, 232001 (2009), 0907.3719.
- [33] J. Braun, A. Eichhorn, H. Gies, and J. M. Pawłowski, Eur. Phys. J. **C70**, 689 (2010), 1007.2619.
- [34] N. Strodthoff, B.-J. Schaefer, and L. von Smekal, Phys. Rev. **D85**, 074007 (2012), 1112.5401.
- [35] A. Dumitru, Y. Guo, Y. Hidaka, C. P. K. Altes, and R. D. Pisarski, (2012), 1205.0137.
- [36] C. Gatttringer, Phys. Rev. Lett. **97**, 032003 (2006), hep-lat/0605018.
- [37] F. Synatschke, A. Wipf, and C. Wozar, Phys. Rev. **D75**, 114003 (2007), hep-lat/0703018.
- [38] E. Bilgici, F. Bruckmann, C. Gatttringer, and C. Hagen, Phys. Rev. **D77**, 094007 (2008), 0801.4051.
- [39] K. Kashiwa, M. Matsuzaki, H. Kouno, Y. Sakai, and M. Yahiro, Phys. Rev. **D79**, 076008 (2009), 0812.4747.
- [40] Y. Sakai, K. Kashiwa, H. Kouno, and M. Yahiro, Phys. Rev. **D77**, 051901 (2008), 0801.0034.
- [41] E. Bilgici *et al.*, Few Body Syst. **47**, 125 (2010), 0906.3957.
- [42] C. S. Fischer, Phys. Rev. Lett. **103**, 052003 (2009), 0904.2700.
- [43] C. S. Fischer and J. A. Mueller, Phys. Rev. **D80**, 074029 (2009), 0908.0007.
- [44] C. S. Fischer, A. Maas, and J. A. Muller, Eur. Phys. J. **C68**, 165 (2010), 1003.1960.
- [45] B. Zhang, F. Bruckmann, C. Gatttringer, Z. Fodor, and K. K. Szabo, (2010), 1012.2314.
- [46] T. K. Mukherjee, H. Chen, and M. Huang, Phys. Rev. **D82**, 034015 (2010), 1005.2482.
- [47] R. Gatto and M. Ruggieri, Phys. Rev. **D82**, 054027 (2010), 1007.0790.
- [48] J. Greensite, Prog. Part. Nucl. Phys. **51**, 1 (2003), hep-lat/0301023.
- [49] F. Karsch and M. Lutgemeier, Nucl. Phys. **B550**, 449 (1999), hep-lat/9812023.
- [50] J. Engels, S. Holtmann, and T. Schulze, Nucl. Phys. **B724**, 357 (2005), hep-lat/0505008.
- [51] E. Bilgici, C. Gatttringer, E.-M. Ilgenfritz, and A. Maas, JHEP **0911**, 035 (2009), 0904.3450.
- [52] H. Nishimura and M. C. Ogilvie, Phys. Rev. **D81**, 014018 (2010), 0911.2696.
- [53] T. Kahara, M. Ruggieri, and K. Tuominen, (2012), 1202.1769.
- [54] K.-I. Kondo, Phys. Rev. **D82**, 065024 (2010), 1005.0314.
- [55] J. Kogut and D. Sinclair, Nucl. Phys. Proc. Suppl. **53**, 272 (1997), hep-lat/9607083.
- [56] S. Catterall, R. Galvez, J. Hubisz, D. Mehta, and A. Veernala, (2011), 1112.1855.
- [57] H. S. Fukano and F. Sannino, Phys. Rev. **D82**, 035021 (2010), 1005.3340.
- [58] L. Del Debbio, A. Patella, and C. Pica, Phys. Rev. **D81**, 094503 (2010), 0805.2058.
- [59] S. Catterall, J. Giedt, F. Sannino, and J. Schneible, JHEP **11**, 009 (2008), 0807.0792.
- [60] L. Del Debbio, B. Lucini, A. Patella, C. Pica, and A. Rago, Phys. Rev. **D80**, 074507 (2009), 0907.3896.
- [61] F. Sannino, Acta Phys. Polon. **B40**, 3533 (2009), 0911.0931.
- [62] D. D. Dietrich and F. Sannino, Phys. Rev. **D75**, 085018 (2007), hep-ph/0611341.
- [63] M. Cheng *et al.*, Phys. Rev. **D81**, 054504 (2010), 0911.2215.
- [64] S. Datta and S. Gupta, Phys. Rev. **D82**, 114505 (2010), 1006.0938.
- [65] S. Borsanyi *et al.*, arXiv:1011.4230, 1011.4230.
- [66] A. Bazavov and P. Petreczky, PoS LATTICE2010, 169 (2010), 1012.1257.
- [67] K. Kanaya, AIP Conf. Proc. **1343**, 57 (2011), 1012.4235.
- [68] V. G. Bornyakov *et al.*, (2011), 1102.4461.
- [69] A. Maas, J. M. Pawłowski, L. von Smekal, and D. Spielmann, (2011), 1110.6340.
- [70] J. Braun, H. Gies, and J. M. Pawłowski, Phys. Lett.

- B684**, 262 (2010), 0708.2413.
- [71] F. Marhauser and J. M. Pawłowski, 0812.1144.
- [72] N. Weiss, Phys.Rev. **D24**, 475 (1981).
- [73] D. J. Gross, R. D. Pisarski, and L. G. Yaffe, Rev.Mod.Phys. **53**, 43 (1981).
- [74] R. D. Pisarski, Phys. Rev. **D62**, 111501 (2000), hep-ph/0006205.
- [75] A. Dumitru, Y. Hatta, J. Lenaghan, K. Orginos, and R. D. Pisarski, Phys.Rev. **D70**, 034511 (2004), hep-th/0311223.
- [76] A. Dumitru, Y. Guo, Y. Hidaka, C. P. K. Altes, and R. D. Pisarski, Phys.Rev. **D83**, 034022 (2011), 1011.3820.
- [77] K. Fukushima, J.Phys.G **G39**, 013101 (2012), 1108.2939.
- [78] C. Sasaki and K. Redlich, (2012), 1204.4330.
- [79] M. Ruggieri *et al.*, (2012), 1204.5995.
- [80] K. Huebner, F. Karsch, O. Kaczmarek, and O. Vogt, Phys.Rev. **D77**, 074504 (2008), 0710.5147.
- [81] S. Gupta, K. Huebner, and O. Kaczmarek, Phys.Rev. **D77**, 034503 (2008), 0711.2251.
- [82] C. Wetterich, Phys. Lett. **B301**, 90 (1993).
- [83] D. F. Litim and J. M. Pawłowski, in *The Exact Renormalization Group*, Eds. Krasnitz et al., World Scientific (1999), hep-th/9901063.
- [84] C. Bagnuls and C. Bervillier, Phys. Rept. **348**, 91 (2001), hep-th/0002034.
- [85] J. Berges, N. Tetradis, and C. Wetterich, Phys. Rept. **363**, 223 (2002), hep-ph/0005122.
- [86] J. Polonyi, Central Eur. J. Phys. **1**, 1 (2003), hep-th/0110026.
- [87] B. Delamotte, D. Mouhanna, and M. Tissier, Phys. Rev. **B69**, 134413 (2004), cond-mat/0309101.
- [88] J. M. Pawłowski, Annals Phys. **322**, 2831 (2007), hep-th/0512261.
- [89] H. Gies, hep-ph/0611146.
- [90] B.-J. Schaefer and J. Wambach, Phys.Part.Nucl. **39**, 1025 (2008), hep-ph/0611191.
- [91] B. Delamotte, cond-mat/0702365.
- [92] O. J. Rosten, Phys.Rept. **511**, 177 (2012), 1003.1366.
- [93] T. Zhang, T. Brauner, and D. H. Rischke, JHEP **1006**, 064 (2010), 1005.2928.
- [94] C. Sasaki, B. Friman, and K. Redlich, Phys. Rev. **D75**, 074013 (2007), hep-ph/0611147.
- [95] A. J. Mizher, M. N. Chernodub, and E. S. Fraga, Phys. Rev. **D82**, 105016 (2010), 1004.2712.
- [96] V. Skokov, B. Stokic, B. Friman, and K. Redlich, Phys. Rev. **C82**, 015206 (2010), 1004.2665.
- [97] V. Skokov, B. Friman, and K. Redlich, Phys.Rev. **C83**, 054904 (2011), 1008.4570.
- [98] B.-J. Schaefer, M. Wagner, and J. Wambach, Phys. Rev. **D81**, 074013 (2010), 0910.5628.
- [99] J. Berges, D. U. Jungnickel, and C. Wetterich, Phys. Rev. **D59**, 034010 (1999), hep-ph/9705474.
- [100] J. Braun, Phys. Rev. **D81**, 016008 (2010), 0908.1543.
- [101] H. Gies, J. Jaeckel, and C. Wetterich, Phys.Rev. **D69**, 105008 (2004), hep-ph/0312034.
- [102] S. R. Coleman and E. Witten, Phys.Rev.Lett. **45**, 100 (1980).
- [103] D. D. Scherer and H. Gies, (2012), 1201.3746.
- [104] K. Fukushima and J. M. Pawłowski, (2012), 1203.4330.
- [105] J. Braun, H. Gies, and D. D. Scherer, Phys. Rev. **D83**, 085012 (2011), 1011.1456.
- [106] R. Alkofer and L. von Smekal, Phys.Rept. **353**, 281 (2001), hep-ph/0007355.
- [107] C. S. Fischer, J.Phys.G **G32**, R253 (2006), hep-ph/0605173.
- [108] A. Maas, 1106.3942.
- [109] C. D. Roberts, 1203.5341.
- [110] H. Gies, S. Rechenberger, and M. M. Scherer, Eur.Phys.J. **C66**, 403 (2010), 0907.0327.
- [111] D. D. Scherer, J. Braun, and H. Gies, (in preparation).
- [112] N. Tetradis and C. Wetterich, Nucl. Phys. **B422**, 541 (1994), hep-ph/9308214.
- [113] C. S. Fischer, J. Luecker, and J. A. Mueller, (2011), 1104.1564.
- [114] D. F. Litim, Phys. Lett. **B486**, 92 (2000), hep-th/0005245.
- [115] D. F. Litim, Int. J. Mod. Phys. **A16**, 2081 (2001), hep-th/0104221.
- [116] D. F. Litim, Phys. Rev. **D64**, 105007 (2001), hep-th/0103195.
- [117] D. F. Litim and J. M. Pawłowski, JHEP **11**, 026 (2006), hep-th/0609122.
- [118] J.-P. Blaizot, A. Ipp, R. Mendez-Galain, and N. Wschebor, Nucl. Phys. **A784**, 376 (2007), hep-ph/0610004.